NATURAL CONVECTION HEAT TRANSFER FROM ROUGHENED INCLINED PLATES FACING UPWARDS

A Thesis Submitted
in Partial Fulfilment of the Requirements
for the Degree of
MASTER OF TECHNOLOGY

By
SUDHAKAR RAMBHAU NARKHEDE

to the
DEPARTMENT OF MECHANICAL ENGINEERING
INDIAN INSTITUTE OF TECHNOLOGY, KANPUR
AUGUST, 1978

To my beloved
MOTHER
who is no more

7.8.70
24

CERTIFICATE

This is to certify that this work on "Natural Convection Heat Transfer from Roughened Inclined Plates Facing Upwards" has been carried out under my supervision and has not been submitted elsewhere for a degree.

P.N.KAUL
Assistant Professor
Department of Mechanical Engineering
Indian Institute of Technology, Kanpur

ACKNOWLEDGEMENTS

I wish to express my deep sense of gratitute to Dr. P.N.Kaul for his invaluable guidance in the initiation, progress and completion of the present study.

I am grateful to Mr. Manohar Prasad and Mr. K.K.Saxena for useful discussions and various suggestions made during the course of this work.

I am very thankful to my friends Mr. A.V.A. Swamy, Mr. Vishwanath Prasad, Mr. R.S. Chaudhary and all other colleagues who helped me directly and indirectly.

I thank Messers P.N. Misra, P.N. Sharma and S.N. Sharma for their help with the fabrication, installation and the commissioning of the experimental facility. My sincere thanks are also due to Mr. D.K. Sarkar for his help in taking the photographs.

Last but not the least, I would like to express my appreciation to Mr. D.P. Saini for his excellent typing.

S.R. Narkhede

(S.R. NARKHEDE)

CONTENTS

LIST OF FIGURES

NOMENCLATURE

A	=	Area of exposed surface, m^2
a	=	Constant in equation, $f = a(e/\delta)^m$
$^\circ C$	=	Degree centrigrade
C_p	=	Specific heat, Kcal/Kg $-^\circ C$
e	=	Absolute roughness, m
f	=	Friction factor
g	=	Gravitational acceleration, m^2/sec
h	=	Local heat transfer coefficient, Kcal/hr-$m^2-^\circ C$
h_{avg}	=	Average heat transfer coefficient, Kcal/hr-$m^2-^\circ C$
K	=	Thermal conductivity of air, Kcal/hr-m-$^\circ C$
$^\circ K$	=	Degree kelvin
K'	=	Dimensionless constant for air
L	=	Length of plate, m
m	=	Exponent in the equation, $f = a\,(e/\delta)^m$
n	=	Refractive index of air
q	=	Power input, watt
q_i	=	Power input, Kcal/hr
q_c	=	Convective heat loss, Kcal/hr
q_r	=	Radiative heat loss, Kcal/hr
t_o	=	Average temperature of the plate, $^\circ C$

t_∞ = Temperature of room air, °C

t_m = Mean film temperature, °C

t_w = Temperature of room walls, °C

T_o = Average temperature of air, °K

T_w = Temperature of room walls , °K

Gr = Grashof number , $g\beta\ (t_o - t_\infty)\ L^3/\ \nu^2$

Pr = Prandtl number, $\mu C_p/K$

Nu = Average Nusselt number, $h_{avg} L/K$

Ra = Rayleigh number, Gr Pr

Greek letters

β = Coefficient of thermal expansion, °K

δ = Boundary layer thickness, m

θ = Inclination of the plate with vertical, degrees

ρ = Density of air, Kg/m^3

ρ_o = Density of air at normal temperature and pressure, Kg/m^3

μ = Absolute viscosity, (Kg/m-hr)

ν = Kinematic viscosity, m^2/sec

ε = Eddy diffusivity, m^2/sec

ε_a = Emissivity of roughened aluminium plate

σ = Stefan-Boltzman constant, $Kcal/hr\text{-}m^2\text{-}°K^4$

ϕ = Nondimensional temperature, $(t - t_\infty)/(t_o - t_\infty)$

τ_w = Wall shear stress, Kg/m^2

ABSTRACT

Natural Convection Heat Transfer from
Roughened Inclined Plates Facing Upwards

Sudhakar Rambhau Narkhede
Master of Technology
Department of Mechanical Engineering
Indian Institute of Technology, Kanpur
August 1978

Natural convection heat transfer from an electrically heated roughened inclined plate (650 X 310 X 12 mm) facing upwards has been studied. An integral method analysis of the problem has been supplemented by an experimental investigation. Based on the experimental data a natural convection heat transfer correlation for the roughened inclined plates facing upwards has been developed, which is

$$Nu = 0.105\ (Ra \cos\theta)^{0.36}$$

Augmentation to the free convective heat transfer due to surface roughness in the present investigation is found to be of the order of 35 percent.

The study also includes the use of schlieren apparatus for flow visualization purposes. Schlieren photograph show the boundary layer build up. The boundary layer is seen to increase in all the cases studied from the leading edge to the trailing edge. However, for the same pitch to height ratio of the roughness and the temperature, the boundary layer thickness is seen to decrease with the increase in height of roughness.

CHAPTER 1

1.1 INTRODUCTION

Free or natural convection is the mode of heat transfer that occurs when a body is placed in a still fluid at a temperature different from that of the body. As a result of the temperature difference density changes take place in the medium surrounding the body. The fluid starts to flow due to the buoyancy forces created by density gradients. In the forced convection heat transfer, however, the flow is imposed and maintained mechanically by means of a pump, a compressor or a blower.

Heat transfer due to free convection plays an important role in many practical engineering applications. Free convection heat losses are commonly encountered in situations like pipes carrying heated fluids, walls and ceilings of buildings, steam radiators, evaporators, condensors and other bodies placed in a quiescent atmosphere at a temperature above or below that of the bodies concerned. Cooling of structural parts in propulsion systems like gas turbine blades, rocket nozzles and combustion chamber walls is also achieved by free convection flows which are produced by centrifugal forces.

Mathematically speaking, Grashof and Prandtl numbers are the two important non-dimensional parameters which characterise the

type of flow in natural convection, while in forced convection, Reynolds number plays a dominant role. Differential equations for velocity and thermal boundary layers are coupled and consequently an interaction exists between the temperature and the velocity fields, making the problem of natural convection analytically more complicated than that of the forced convection. Moreover, if there exist large temperature gradients within the fluid, variation of properties other than density, like, thermal conductivity and viscosity should also be taken into account to make an appropriate analytical study of the flow. Hence, both the momentum and the energy equations have to be solved simultaneously in any study of the natural convection problem. Their solutions, however, are tedious and complicated, if not impossible.

Many natural convection phenomena are therefore investigated experimentally to avoid the difficulties inherent in obtaining an analytical solution.

1.2 REVIEW OF PREVIOUS WORK

Interest in natural convection on inclined surfaces arose out of attempts to describe thermal stratification in insulated cryogenic propellant vessels, where a substantial amount of heat transfer takes place through the bottom of the vessel. Rich (1) made both local heat transfer and boundary layer temperature measurements in laminar region on an inclined plate facing upwards. The plate, 4 - in wide, 16 - in

long, $\frac{1}{8}$ - in thick and made of aluminium was heated by means of an electrofilm resistance heating element. No constant voltage transformer was used during the tests. Experiments were carried out in an air-conditioned room, so that the ambient temperature could be maintained constant. Angles of inclination of the test plates ranged from 0 to 40 degrees, measured from the vertical. Rich conjectured theoretically that the heat transfer coefficient for an inclined heated plate could be treated just as for a vertical plate, if the gravitational term in Grashof number was altered to the component parallel to the inclined surface.

Vliet (2) made experimental study of local heat transfer coefficients on a constant heat flux inclined surface facing upwards. The plate which was 4 feet long and 3 feet wide was energized by an electrically heated .002-in thick stainless steel sheet. The plate was immersed and tested in a constant temperature water bath. The boundary layer flow was two dimensional. To have a consistent leading-edge condition for the whole range of plate inclinations, a right-angle geometry was maintained near the plate leading edge by attaching a wall perpendicular to the plate. Experiments were performed with the plate inclined at a range of angles varying between 30 to 85 degrees with the horizontal.

Fujii and Imura (3) made an experimental study of natural convection heat transfer from a plate with arbitrary inclination.

A plate made of brass of 30 cm length, 15 cm width and 1 cm thickness was heated by a sheath heater of 2.3 mm diameter, which was buried with 6 mm pitch in a solder sheet. The main flow in the boundary layer was restricted to two-dimensions only. Correlations have been presented for both the cases i.e. the inclined plate facing downwards and the inclined plate facing upwards. Fujii and Imura found that for the inclined plate facing downwards the wall temperature increased sharply with the distance from the leading edge. This was caused mainly by the variation of the local heat transfer coefficient and by the stratification of the fluid temperature. The authors also observed that for the inclined plate facing upwards the wall temperature was far more uniform than that for the inclined plate facing downwards, because the boundary layer flow in the former case was susceptible to instability and gave way to turbulence.

Black and Norris (4) studied the thermal structure of free convection turbulence from isothermal inclined surfaces. A Differential interferometer was used to provide flow visualization and to measure the local heat transfer coefficients. The test assembly consisted of an aluminium plate 1.27 cm thick and 152 x 25.4 cm^2 surface area. The plate was heated by ten segmented electrical heaters attached to the rear surface of the plate. Side barriers were placed along the entire plate length to prevent room air currents from disturbing the measurements. Black et al found that data in the turbulent regime

were insensitive to the plate inclination and distance from the leading edge of the plate.

A comprehensive study of the effect of surface roughness on friction and velocity distribution was performed by Nikuradse (5). In contrast to this, very thorough and complete experimental work, the study of the effect of roughness on heat transfer has received relatively very little attention.

Boelter et al (6) presented heat transfer data for a system in which air was passed over a heated flat plate containing strips of metal placed normal to the direction of air flow. Two heights of interrupters or strips (1/8-in and 3/8-in) were used and mounted at 1 in pitch. These boundary layer interrupters acted as turbulence promoters. Boelter et al found that the heat transfer rates of roughened plates were increased from 50 to 200 percent over that for the flat plate alone.

Nunner (7) made an extensive study of the convective heat transfer to the moving air within a tube roughened artificially from inside, by pushing spring rings into a smooth tube. The main conclusion of Nunner's work are, however, open to question. He measured the velocity distribution at the exit end of the experimental tube by means of a 1mm diameter Pitot tube. Nunner's measurements showed that with equal Reynolds numbers the velocity profile was more drawn out in the case of the rough tube than with the smooth. Nunner extrapolated

his results to the region close to the wall and came to the conclusion that the laminar sublayer thickens as a result of surface roughness. On the other hand he took into account the possibility of the breakdown of the laminar sublayer on the roughness asperities, and then taking into account all these factors came to the conclusion that the laminar sublayer was the same in both the rough and the smooth tubes. By combining the velocity and the temperature profiles on the rough tube Nunner also came to believe that the effect of surface roughness on heat transfer was similar to the effect of increasing the Prandtl number.

Edwards and Sheriff (8) studied the effect, on the local heat transfer coefficient, of transverse wires fixed to a flat heating surface for a two-dimensional turbulent air flow. The wires were of circular cross-section and were attached to the surface at right angles to the fluid flow. For a single wire to become fully effective in improving the heat transfer the authors suggest that the height of the wire must exceed about twice the laminar sublayer thickness before it produces any significant effect. Its effect increases as it penetrates the buffer layer and it becomes fully effective when its height exceeds the overall thickness of the combined sublayer and the buffer layer. They also found with their multi-wire tests, that the improvement in heat transfer was very "peaked". Gomelauri (9) investigated the effect of artificial surface roughening on heat transfer between a wall and a turbulent flowing liquid. He carried out tests

on electrically heated tubes,roughened either by machining on a lathe or by lead-soldering to the surface 0.68 mm nichrome wire in the form of rings. The heated tubes were located axially within a circular channel of 33 mm internal diameter . Heat from the rough surfaces was transmitted to the liquid flowing along the annular channel. Gomelauri developed an empirical relation by correlating his own and other author's experimental data to predict the mean coefficient of heat transfer for artificially roughened surfaces in a turbulent fluid stream.

Sheriff et al (10) studied heat transfer characteristics of roughened surfaces. Their test set up comprised an annulus with an inner and outer tube diameters of 1-in and 2-in respectively. The central core of the annulus formed the heater element and the inner surface of the annulus was the test surface,nominally of 1-in outside diameter with a wall thickness of 0.1-in . The surface of this heater tube was machined to give the square roughness elements of various pitch to height ratios. The roughness heights were chosen so that at the lowest Reynolds number tested the laminar sublayer would be of the same order as the roughness height. The range of Reynolds numbers studied varied from 10^4 to 10^5. Sheriff et al found that heat transfer increased with the increase in the pitch to height ratio of roughness. They also observed that friction factor increased with the increase in the roughness height for the same pitch to height ratio.

Gowen and Smith (11) studied turbulent heat transfer from smooth and roughened tubes. They carried out experiments on an internally roughened 2-in I.D. brass tube, 24-in long with water and 30% aqueous ethylene glycol solution passing through it. The wall of the brass tube was roughened by tinning and then soldering a 12 mesh brass screen to the inside surface of the pipe. The heating section was made by concentrically placing the brass pipe in a 2.625-in O.D. copper tube and pouring molten solder in the annulus. The outside surface was covered with a thin layer of Teflon film and then uniformly wrapped with a nichrome ribbon resistance heater. Their findings showed that for the same Reynolds number, the Stanton number for the roughened pipes was much higher than that for the smooth pipes.

1.3 SCOPE OF THE PRESENT WORK

In many of the industrial problems, pertaining to the design of thermal equipment, optimisation of the heat transfer surface plays an important role. The development of high performance thermal systems has also stimulated interest in methods to enhance or intensify heat transfer from thermal devices. The performance of conventional heat exchangers can be substantially improved by a number of augmentative techniques.

Surface roughness was one of the first technique to be considered seriously as a means of augmenting heat transfer. Since the commercial roughness is not well defined, artificial surface

roughness has been generally employed in testing surfaces. In forced convective problems several types of surface roughnesses have been investigated to arrive at the best configuration of the roughness, treating the thermal energy dissipation per unit pumping horse power as an index signifying the efficiency of the transport phenomena.

However, very little data are available regarding the free convective heat transfer from roughened surfaces. Free convective heat transfer from several geometries such as a cylinder, a sphere and an inclined flat plate have been investigated both for the laminar and the turbulent flow regimes. In all these cases the surfaces have been invariably assumed to be smooth from the microscopic point of view.

It was against this background, that the present study into the effect of artificial surface roughness on natural convection heat transfer from an inclined flat plate, facing upwards, was undertaken. The data obtained from this investigation can be helpful in predicting the heat transfer characteristics of roughnened flat plates facing upwards for cooling or heating purposes under similar and moderately varied conditions.

CHAPTER 2

THEORETICAL ANALYSIS

Momentum and energy equations for an inclined flat plate can be transformed into an integro-differential form with the help of the law of continuity. The velocity and the temperature profiles can be obtained by postulating a suitable expression for the eddy diffusivity. Since the mechanisms of thermal and momentum diffusion near about a solid boundary having certain roughness characteristics are not conclusively known, Ede (12) demonstrated that an eddy diffusivity expression like $\varepsilon/\nu = .4y^{+}\left[\,1 - \exp\left(-\,0.0017y^{+2}\right)\,\right]$, valid for $0 \leq y^{+} \leq \infty$, can be utilized to predict successfully the turbulent free convective heat transfer from a vertical plate.

Solutions to the problems of turbulent free convection flow have also been attempted by assuming appropriate shapes for the temperature and velocity distributions in the free convection boundary layer. This approach adopted by Eckert and Jakson (13) in their analysis of turbulent free convection boundary layer on a flat vertical plate has yielded satisfactory results. In the present analysis also the same method has been used.

Evaluation of wall shear stress poses certain problems for the rough surfaces. Forced convective flow over rough flat surfaces,

as studied by Nikuradse, indicates that the friction coefficient remains independent of the Reynolds number of the flow, but is very much dependent on the absolute roughness factor 'e'. For the case of the forced flow over a rough plate, Nikuradse, recommended the following expression for the determination of the friction coefficient.

$$f = (1.89 + 1.62 \log \delta/e)^{-2.5}$$

Similarly, Hopf (14) and Fromm (15) found out that resistance to flow in rough channels (roughened by wire nets, serrated zinc sheets and corrugated steel) is a function of the absolute roughness factor. They expressed the friction factor for a rough surface as , $f = 0.01 (e/r_w)^{0.314}$.

Such a universal character can also be anticipated for the free convective flow along inclined roughened surfaces. Hence in the analysis of the free convective problem also the friction coefficient 'f' could be assumed to be given by an expression of the form,

$$f = a (e/\delta)^m$$

where a and m are two unknown constants and δ is the thickness of the thermal boundary layer.

By dimensional analysis for the problem under consideration the governing system of criteria can be expressed as

$$Nu = F (Gr , Pr , e/\delta , \theta)$$

Considering an inclined surface as shown in Figure (2.1).

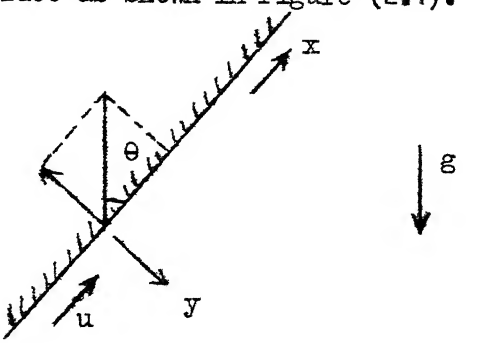

Fig. 2.1 Inclined plate geometry

As the surface is inclined to the local direction of the gravity field the buoyancy force causing motion has a component in the flow in both the tangential and the normal directions.

Local buoyancy force	=	$g \beta \rho(t-t_\infty)$
Component of the buoyancy force in the tangential direction	=	$g \beta \rho(t-t_\infty) \cos\theta$
Component of the buoyancy force in the normal direction	=	$g \beta \rho(t-t_\infty) \sin\theta$

Thus the boundary layer equations for a two dimensional flow with the above body force contributions and the boundary-layer approximations are modified to yield

$$u \frac{\partial u}{\partial x} + v \frac{\partial u}{\partial y} = \nu \frac{\partial^2 u}{\partial y^2} + g\beta (t-t_\infty) \cos\theta - \frac{1}{\rho} \frac{\partial p_m}{\partial x} \qquad (2.1)$$

1 1 δ 1/δ 1 1

$$u \frac{\partial v}{\partial x} + v \frac{\partial v}{\partial y} = \nu \frac{\partial^2 v}{\partial y^2} + g\beta (t-t_\infty) \sin\theta - \frac{1}{\rho} \frac{\partial p_m}{\partial y} \qquad (2.2)$$

1 δ δ 1 δ 1

where

p_m (Motion pressure) = Total pressure (p) - Hydrostatic pressure (p_h)

Equations 2.1 and 2.2 are written for constant viscosity, μ.

From the boundary layer order of magnitude analysis, the order of the magnitude of the various terms for the generalised form of the equations can be known. Therefore neglecting the terms of order of δ (the boundary layer thickness). Equations 2.1 and 2.2 reduce to

$$u\frac{\partial u}{\partial x} + v\frac{\partial u}{\partial y} = \nu\frac{\partial^2 u}{\partial y^2} + g\beta(t-t_\infty)\cos\theta - \frac{1}{\rho}\frac{\partial p_m}{\partial x} \qquad (2.3)$$

$$0 = g\beta(t-t_\infty)\sin\theta - \frac{1}{\rho}\frac{\partial p_m}{\partial y} \qquad (2.4)$$

From equation (2.4), the pressure term turns out to be of order 1. p_m, therefore, must be of order δ as y is of order δ. The pressure term in equation (2.3) therefore being only of negligible order δ can be ignored to give

$$u\frac{\partial u}{\partial x} + v\frac{\partial u}{\partial y} = \frac{1}{\rho}\frac{\partial \tau}{\partial y} + g\beta(t-t_\infty)\cos\theta \qquad (2.5)$$

For the energy equation

$$u\frac{\partial t}{\partial x} + v\frac{\partial t}{\partial y} = \frac{K}{\rho C_p}\frac{\partial^2 t}{\partial y^2}$$

Let $$\phi = \frac{(t-t_\infty)}{(t_o-t_\infty)} = \frac{(t-t_\infty)}{\Delta T}$$

The equation then becomes

$$u\frac{\partial \phi}{\partial x} + v\frac{\partial \phi}{\partial y} = \frac{K}{\rho C_p}\frac{\partial}{\partial y}\left(\frac{\partial \phi}{\partial y}\right) \qquad (2.6)$$

As $$q = -K \frac{\partial}{\partial y}(t - t_\infty) = \frac{-K}{\Delta T} \frac{\partial \phi}{\partial y}$$

Equation (2.6) further yields,

$$u \frac{\partial \phi}{\partial x} + v \frac{\partial \phi}{\partial y} = -\frac{1}{\rho C_p \Delta T} \frac{\partial q}{\partial y} \qquad (2.7)$$

From the continuity equation

$$\frac{\partial u}{\partial x} + \frac{\partial v}{\partial y} = 0$$

we get $$\partial v = -\frac{\partial u}{\partial x} \partial y \qquad (2.8)$$

Equation (2.5) on integration gives

$$\int_0^\delta u \frac{\partial u}{\partial x} \partial y + \int_0^\delta v \partial u = \frac{1}{\rho} \int_0^\delta \partial \tau + g\beta \Delta T \cos\theta \int_0^\delta \phi \partial y$$

$$\int_0^\delta u \frac{\partial u}{\partial x} \partial y + u v \Big|_0^\delta - \int_0^\delta u \partial v = -\frac{1}{\rho} \tau_w + g\beta \Delta T \cos\theta \int_0^\delta \phi \partial y$$

$$2 \int_0^\delta u \frac{\partial u}{\partial x} \partial y = \frac{\partial}{\partial x} \int_0^\delta u^2 \partial y = -\frac{\tau_w}{\rho} + g\beta \Delta T \cos\theta \int_0^\delta \phi \partial y$$

$$\frac{\partial}{\partial x} \int_0^\delta u^2 \partial y = -\frac{\tau_w}{\rho} + g\beta \Delta T \cos\theta \int_0^\delta \phi \partial y \qquad (2.9)$$

Also equation (2.7) on integration becomes

$$\int_0^\delta u \frac{\partial \phi}{\partial x} \partial y + \int_0^\delta v \partial \phi = \frac{q_w}{\rho C_p \Delta T}$$

$$\int_0^\delta u \frac{\partial \phi}{\partial x} \partial y + v \phi \Big|_0^\delta - \int_0^\delta \phi \partial v = \frac{q_w}{\rho C_p \Delta T}$$

$$\int_0^\delta u \frac{\partial \phi}{\partial x} \partial y + \int_0^\delta \phi \frac{\partial u}{\partial x} \partial y = \frac{q_w}{\rho C_p \Delta T}$$

$$\frac{\partial}{\partial x} \int_0^{\delta} u \rho \phi \, \partial y = \frac{q_w}{\rho C_p \Delta T} \qquad (2.10)$$

To solve equations 2.9 and 2.10 the velocity and the temperature distributions may be taken as given by the following equations respectively.

$$\frac{u}{u_1} = (y/\delta)^{1/7} (1 - y/\delta)^4 \qquad (2.11)$$

$$\phi = \frac{(t-t_\infty)}{(t_o-t_\infty)} = 1 - (y/\delta)^{1/7} \qquad (2.12)$$

Equations (2.9) and (2.10) in view of the assumed velocity and temperature profiles get reduced to the following forms

$$.433 \frac{\partial}{\partial x} (u_1^2 \delta) = - 8 \frac{\tau_w}{\rho} + g\beta \delta \Delta T \cos\theta \qquad (2.13)$$

$$.0732 \frac{\partial}{\partial x} (u_1 \delta) = \frac{q_w}{\rho C_p \Delta T} \qquad (2.14)$$

Shear stress at the wall, $\tau_w = \rho u_1^2 f/2$

From Reynolds analogy, $\frac{q_w}{\tau_w} = \frac{C_p \Delta T}{u_1} Pr^{-2/3}$

Substituting the above expressions for τ_w and q_w in equations 2.13 and 2.14 give

$$.433 \frac{\partial}{\partial x} (u_1^2 \delta) = - 8 u_1^2 f/2 + g \beta \Delta T \delta \cos\theta$$

or

$$.433 \frac{\partial}{\partial x} (u_1^2 \delta) = - 4 u_1^2 f + g \beta \Delta T \delta \cos\theta \qquad (2.15)$$

$$.0732 \frac{\partial}{\partial x} (u_1^2 \delta) = \frac{u_1 f}{2} Pr^{-2/3} \qquad (2.16)$$

The friction factor f, the arbitrary velocity function u_1 and the

boundary layer thickness δ may respectively be represented by the expressions given below

$$f = a\,(e/\delta)^m$$

$$u_1 = c_1 x^n \,, \quad \delta = c_2 x^p$$

Substituting the above expressions into equations 2.15 and 2.16 we get

$$.433\,(2n + p)\,x^{2n+p-1}\,c_1^2\,c_2 = \frac{-4\,c_1^2\,x^{2n}\,a\,e^m}{c_2^m\,x^{mp}} + c_2\,g\,\beta\,\Delta T\,x^p\cos\theta \qquad (2.17)$$

$$.0732\,(n + p)\,x^{n+p-1}\,c_1\,c_2 = \frac{1}{2}\,\frac{c_1}{c_2^m}\,\frac{x^n\,a\,e^m}{x^{mp}}\,Pr^{-2/3} \qquad \ldots \quad (2.18)$$

As the above equations 2.17 and 2.18 must be valid for any arbitrary values of x, therefore, the exponents of x on either side of the above equations must be identical.

Therefore

$$2n + p - 1 = 2n - mp = p$$

$$n + p - 1 = n - mp$$

which gives

$$p = \frac{1}{1+m} \quad \text{and} \quad n = 1/2$$

Substituting the above values of p and n into equations 2.17 and 2.18 and solving for c_1 and c_2 we get,

$$c_2 = \left[\,13.66\,\frac{(1+m)}{(3+m)}\,a\,e^m\,Pr^{-2/3}\,\right]^{1/(1+m)}$$

$$c_1 = \left[\frac{g\beta\ \Delta T \cos\theta}{.433\ \frac{(2+m)}{(1+m)} + \frac{4}{13.66}\ \frac{(3+m)}{(1+m)}\ Pr^{2/3}} \right]^{1/2}$$

Heat flow from the wall is given by

$$q_w = h\Delta T = \frac{\tau_w C_p \Delta T}{u_1} Pr^{-2/3}$$

Therefore, $h = \frac{\rho u_1 f C_p}{2} Pr^{-2/3}$

$$h_{avg} = \frac{1}{L} \int_0^L h\, dx$$

$$= \frac{1}{L} \int_0^L \frac{\rho u_1 a (e/\delta)^m C_p}{2} Pr^{-2/3}\, dx$$

$$= \frac{1}{L} \int_0^L \frac{\rho a C_p c_1 e^m}{2 c_2^m} Pr^{-2/3} \left[\frac{1}{2} - \frac{m}{(1+m)}\right] dx$$

$$= \frac{1}{L} \frac{\rho a C_p c_1 e^m}{2 c_2^m} Pr^{-2/3} \left[\frac{3}{2} - \frac{m}{(1+m)}\right] 2 \frac{(1+m)}{(3+m)}$$

$$= \frac{1}{L} \frac{c_1 (1+m)}{c_2^m (3+m)} \rho C_p a e^m Pr^{-2/3} \left[\frac{3}{2} - \frac{m}{(1+m)}\right]$$

Therefore

$$Nu = \frac{h_{avg} L}{K}$$

$$= \frac{c_1}{c_2^m} \frac{(1+m)}{(3+m)} \frac{\rho C_p a e^m}{K} Pr^{-2/3} \left[\frac{1}{2} - \frac{m}{(1+m)}\right]$$

Multiplying and dividing by μ

$$Nu = \frac{c_1}{c_2^m} \frac{(1+m)}{(3+m)} \frac{a\, e^m}{\nu} Pr\, Pr^{-2/3}\, L^{\left[\frac{1}{2} - \frac{m}{(1+m)}\right]}$$

Substituting for c_1 and c_2 we get,

$$Nu = \frac{(1+m)}{(3+m)} a\, e^m\, Pr^{1/3} \left[\frac{g\beta\Delta T \cos\theta\, L^3}{\nu^2 \left[.433 \frac{(2+m)}{(1+m)} + \frac{4}{13.66} \frac{(3+m)}{(1+m)} Pr^{2/3} \right]} \right]^{1/2}$$

$$X \frac{L^{-m/(1+m)}}{c_2^m}$$

$$= \frac{(1+m)}{(3+m)} \frac{\left[.433 \frac{(2+m)}{(1+m)} + \frac{4}{13.66} \frac{(3+m)}{(1+m)} Pr^{2/3} \right]^{-1/2} a\, e^m}{\left[13.66 \frac{(1+m)}{(3+m)} a\, e^m\, Pr^{-2/3} \right]^{m/(1+m)}}$$

$$X\ Pr^{1/3}\, Gr^{1/2}\, (\cos\theta)^{1/2}\, L^{-m/(1+m)}$$

$$= A\, (e/L)^{m/(1+m)}\, Gr^{1/2}\, (\cos\theta)^{1/2} \quad - - - - \quad (2.19)$$

where

$$A = \frac{(1+m)}{(3+m)} \frac{\left[.433 \frac{(2+m)}{(1+m)} + \frac{4}{13.66} \frac{(3+m)}{(1+m)} Pr^{2/3} \right]^{-1/2} a^{1/(1+m)}}{\left[13.66 \frac{(1+m)}{(3+m)} \right]^{m/(1+m)}}$$

$$X\ Pr^{(1+3m)/3(1+m)}$$

CHAPTER 3

3.1 EXPERIMENTAL APPARATUS AND INSTRUMENTATION

The test specimen comprised a rectangular aluminium plate, 65 cm long, 31 cm wide and 1.2 cm thick. The plate was heated by six heating rods placed in an equal number of 1 cm wide semi-circular grooves, 65 cm long, cut along the back of the test plate, with a pitch of 4.4 cm. For minimising the heat losses from the rear of the test plate a guard heater was employed. The guard heater, which was similar in detail to the main heater, was covered by two insulating sheets of asbestos 0.8 and 0.5 cm thick. Sandwiched between the guard heater and the main heater are two asbestos sheets of 0.8 cm thickness. The above units were assembled and bound together by a nut and bolt arrangement, prior to being placed in a wooden box type case filled with glass wool, to keep down the losses from the back of the test plate. With this arrangement only the test surface of the plate and a small portion from the sides was left open to ambient environment. The whole assembly was suspended from a slotted angle frame fitted with castor wheels. To obtain different orientations to the vertical of the test plate for purposes of experimental investigation a system was improvised which consisted of three eye bolts and a wire rope arrangement. The three eye bolts were fastened to the back of the test plate, and were used

to suspend the assembled test specimen from the slotted angle frame in addition to obtaining the desired inclinations of the test plate to the vertical.

Temperature of the test surface was measured with the help of twenty seven 30 SWG Chromel-Alumel thermocouples. To attach the thermocouples to the plate surface the following technique was adopted. Three mm diameter and 11.5 mm deep holes were drilled in the plate from its back face and thermocouple hot junction beads were placed in the holes and fixed into position with the help of Sauereisen number DW-30 cement (a quick setting, electrically insulating but heat conducting cement). Figure (3.1.1) shows the details of the thermocouple locations. Two thermocouples B and B ' were attached to the either side of the asbestos insulation separating the guard and the main heaters, to monitor the temperature difference between the two faces, with a view to exercising an effective control over the back heat losses from the plate. The arrangement can be seen in Figure (3.1.2). Temperature of the sides of the plate was indicated with the help of another seven thermocouples.

The test specimen were roughened artificially by stretching small diameter wires (18 and 16 gauge) across the test plate width along its entire length. To hold the wires in position and in good thermal contact with the plate surface the following procedure was employed. Strips of wood .5 cm thick, 2.5 cm wide and 70 cm long

NOTE- All dimensions are in mm

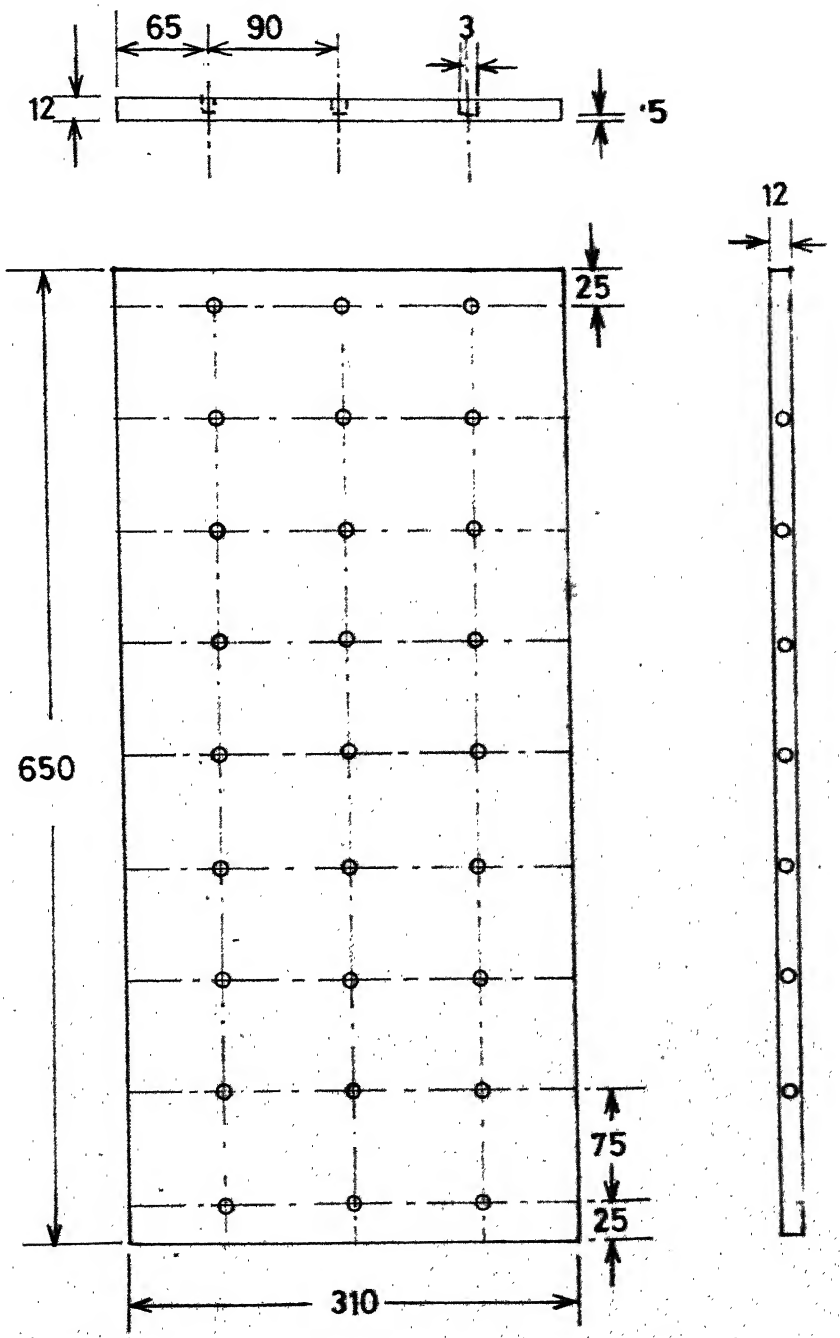

Fig. 3·1·1 Position of thermocouples on the test plate

Note : All dimensions in mm

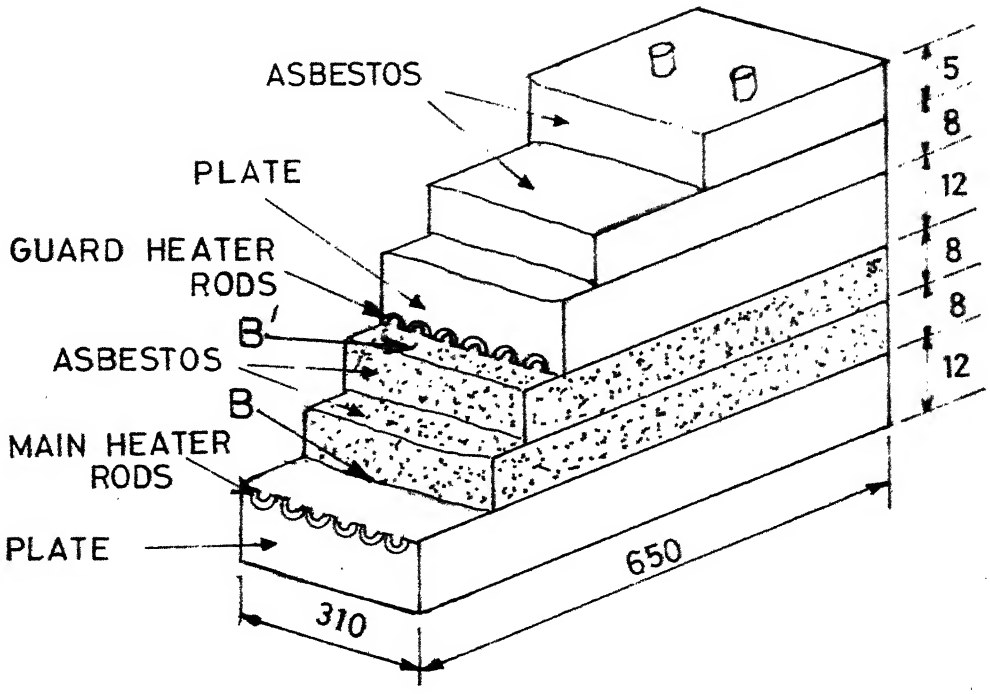

Fig. 3-1-2 Test plate assembly

were nailed to sides of the wooden box containing the test plate assembly. The wires were then wound arround the nails fixed to the sides of the test plate assembly. To maintain good thermal contact between the wires and the test surface the wires were bent along the sides of the test surface for a short distance and glued to the sides with Araldite. This method also ensured that the pitch of wires was uniform. The pitch to height ratio for both the roughnesses was the same.

Stabilized A.C., employing a servo-controlled single-phase voltage stabilizer with an accuracy of $\pm$ 0.1 percent was used to energize both the heaters viz. the main and the guard. The supply was controlled with the help of two auto-transformers and the energy input was recorded by means of a wattmeter with an accuracy of $\pm$ 1%.

The temperature difference between the thermocouples B and B' was maintained within .25^{o}C and controlled by regulating the electric input to the guard heater. Thermocouple readings were measured with a millivolt potentiometer (Leeds and Northrup, No. 8686). The potentiometer was connected to various thermocouples through a number of selector switches. The circuit diagram for thermocouple connections is shown in Figure (3.1.3).

The test plate was mounted in a system, which besides allowing the plate to be held at any desired inclination to the vertical, as mentioned earlier, also permitted the test plate to be moved in

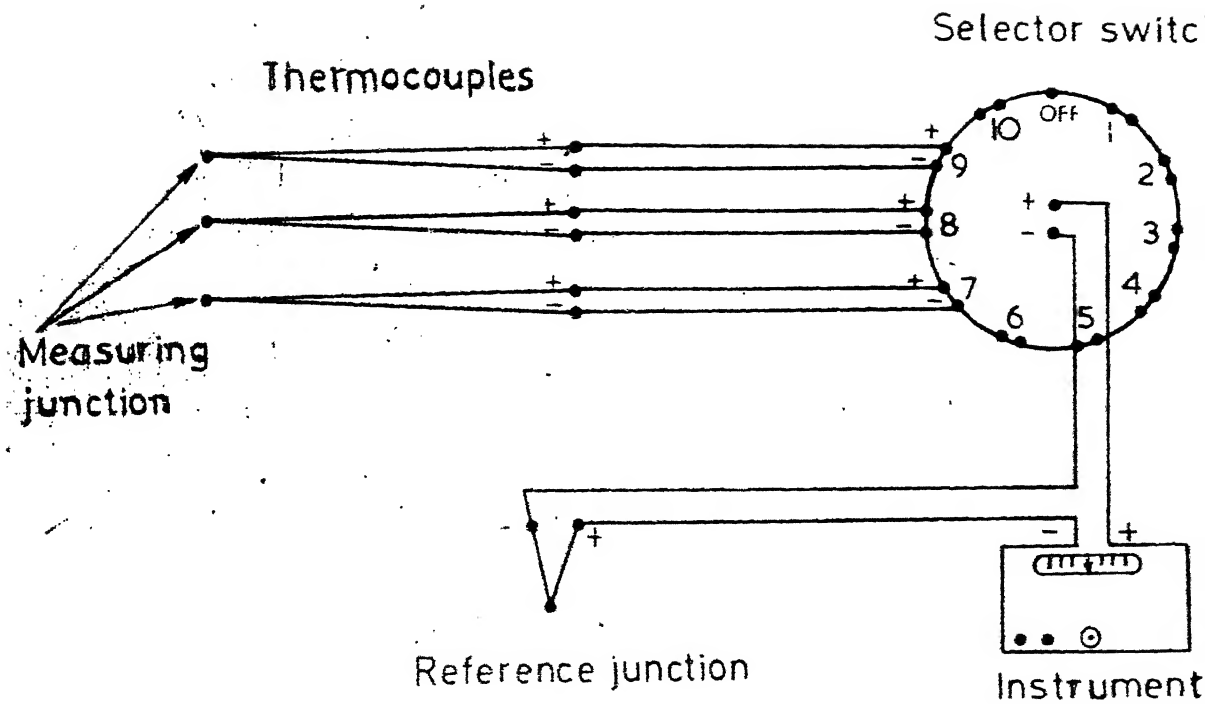

Fig. 3.1.3 Thermocouple connections

and out of the optical zone of the schlieren apparatus for flow visualization purposes. For correct and accurate orientations of the test plate a 12-inch spirit level and a vernier protractor of 1 minute accuracy were used as and when required.

3.2 SCHLIEREN METHOD

3.2.1 Introduction

Numerous methods are available to visualize the flow past models under test. These include the use of tufts, smoke, and oil film placed on the surface of the model, and the vapour-screen and tuft-grid techniques for observing the vortex pattern behind the model. Among these techniques the Schlieren method is most extensively used in high speed and slow speed boundary layer flows, as well as in natural and forced convection heat transfer studies.

This method gives a picture of the flow, caused by changes of refractive index, due to density variations in the flow past the model. The refractive index, n, of the gas is related with sufficient accuracy to its density, ρ , by the equation

$$n - 1 = K' \rho$$

where K' is a constant for a particular gas and for a particular wavelength of light. For air, the equation can be conveniently written as

$$n - 1 = K' \rho / \rho_0 ,$$

where ρ_0 is the density at normal temperature and pressure. The factor k' is dimensionless, and for air, varies between .000290 and .000298 for the visible light spectrum.

If in the working section, there is a gradient of refractive index normal to the light rays, the rays will be deflected as the light travels more slowly where the refractive index is larger as given by the equation:

$$C = C_{va}/n ,$$

C_{va} being the velocity of light in vacuum. The deflection of light rays is a measure of the first derivative of density with respect to distance i.e. the density gradient. The variation of refractive index gradient normal to the rays will differ, so that they will converge or diverge, giving increased or decreased illumination on the screen.

In this work the schlieren technique has been used to visualize flow pattern on a heated roughened plate facing upwards and inclined at angles of 0, 10 and 45 degrees to the vertical. The method yields a qualitative picture of the various regions of density changes in a fluid flowing past a model.

3.2.2 Arrangement of the Apparatus

The apparatus used for the present work is shown in Figure (3.2.1). The light source, S, is placed at the focus of concave mirror, M_1, so that the working section is illuminated by a parallel beam of light. A plane mirror, P_1, has been introduced into the path of the

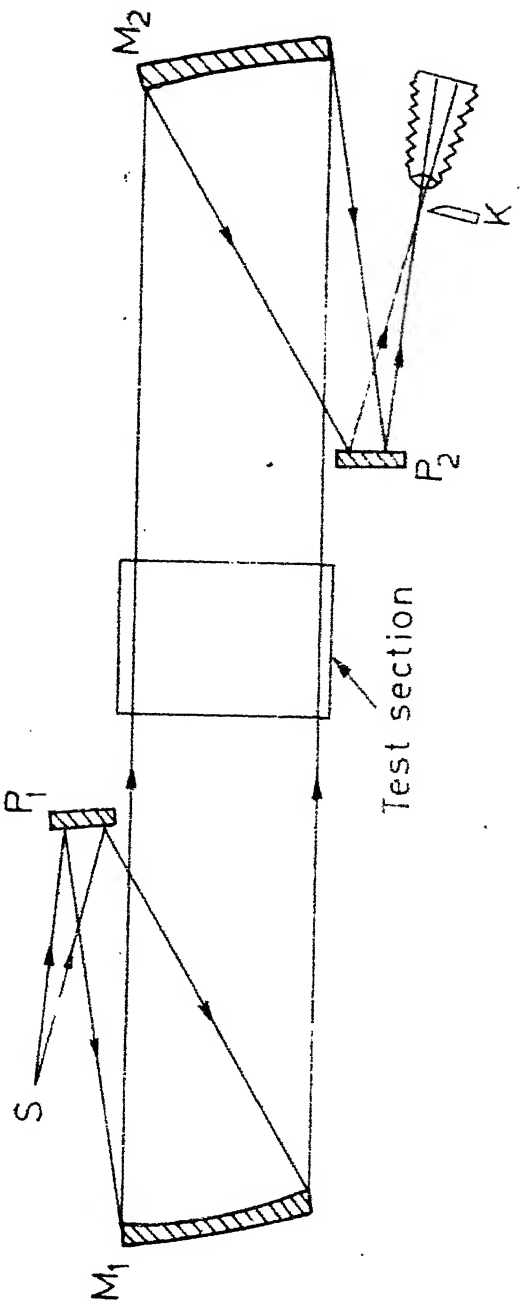

Fig. 3.2.1 Schematic diagram of schlieren apparatus

beam between S and M_1 to fold the light beam. A second concave mirror, M_2 , placed beyond the working section, produces an image of the source in its focal plane, K, and there the knife-edge is introduced. Again the second plane mirror, P_2 , is used to fold the beam emerging from the mirror, M_2.

3.2.3 Apparatus Setting

The procedure for setting up the schlieren system is simple, but depends to some extent on the nature and arrangement of the apparatus and on the type of flow which is to be observed. For the present work with the above described arrangement, the following procedure was adopted.

The first adjustment that is made is to locate the light source, S, at the focus of the first mirror, M_1. The mirror P_1, is adjusted such that the beam of light emerging from S and received by it, is directed towards the mirror M_1 to fill its aperture completely. Now the mirror M_1 is adjusted with the help of screws attached at its back to direct a parallel beam of light through the working section. To facilitate the location of S at focus of mirror M_1, a plane mirror is held between, M_1 and M_2 so as to redirect the beam of light back along its path, from M_1 to P_1, and then to S. An image of S is thus obtained, very close to the original source. If the size of the image is the same as that of the true source, one is sure that S is at the focus of mirror M_1.

The second mirror, M_2, is next moved laterally or vertically until it is filled by the parallel beam emerging from the working section, and is rotated until the light reflected from it, is received by the plane mirror, P_2. Then the mirror P_2 is adjusted to direct the beam of light through the knife-edge assembly.

The knife-edge is now inserted in the focal plane of second mirror and is adjusted until the screen darkens as uniformly as possible when the knife-edge is traversed across the image of the light source. The knife-edge is then so set that a certain fraction of the image of the source is cut off. Now the apparatus is ready for the visualisation of flow patterns around the model introduced into the working section.

3.3 EXPERIMENTAL PROCEDURE

The test plate assembly is suspended by wires from the mobile slotted angle iron frame. The wire ropes are connected to the test assembly through an adjustable hook and eye bolt arrangement. The desired inclination of the test plate to the vertical is obtained by adjusting the lengths of the wire ropes as shown in Figure (3.3.1). Next the power is switched on to the main and the guard heaters and the plate is allowed to reach a steady state condition. Steady state condition is thought to have been reached when the change in temperature of the plate surface is within $1\,^{\circ}C$ per hour. To keep down the heat losses from the back side of the heated plate to the minimum the

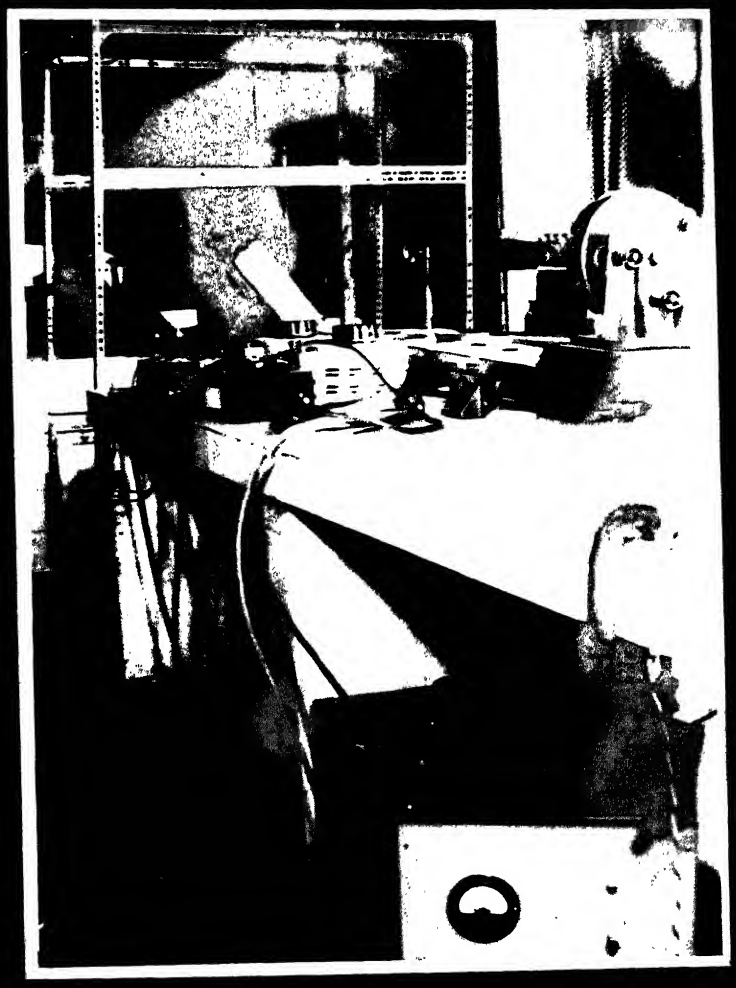

Fig. 3.3.1 Photograph showing the test plate in the test section

difference between the readings of the thermocouples B and B' ,attached to the either side of the asbestos insulation ,separating the main and the guard heaters, as mentioned earlier, is maintained as small as possible. Since there is no a priori way of knowing what combination of electrical inputs to the two heaters viz., the main and the guard, would make the readings of thermocouples B and B' very nearly identical the method adopted for this purpose had to be one of trial and error. It took nearly 6 to 8 hours for the test plate assembly to reach steady state conditions. Once the steady state is reached the readings of all the indicating instruments namely, millivolt potentiometer, wattmeter and thermometer are recorded.

The ranges of various inclinations from the vertical, surface conditions and power dissipations for which experiments were carried out on the test plate assembly are given in Table 1.

For flow visualization purposes the test specimen under various conditions of inclination and surface roughness were examined on the schlieren apparatus. The schlieren photographs are shown in Figures 3.3.2 and 3.3.3.

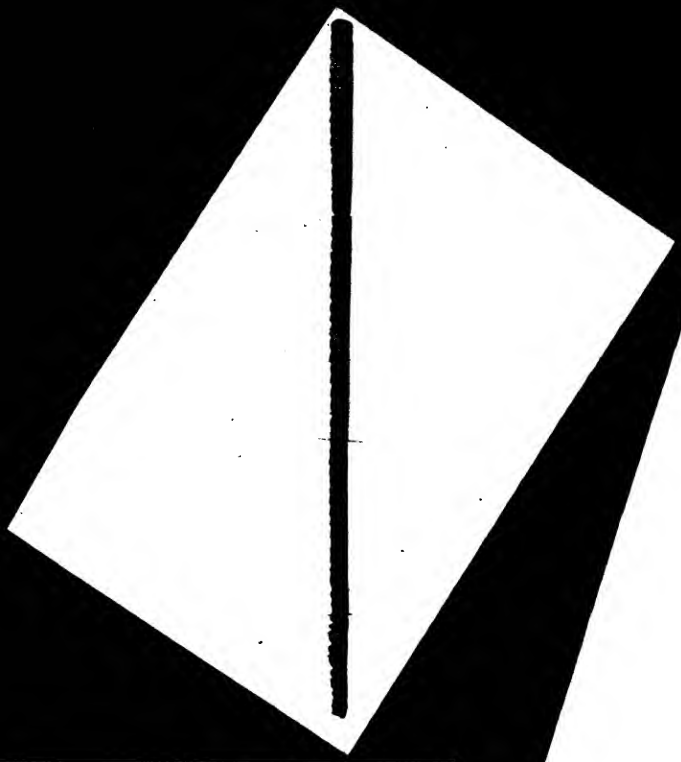

(a) $\theta = 0^{\circ}$, $t_o = 114^{\circ}C$

(b) $\theta = 10^{\circ}$, $t_o = 114$

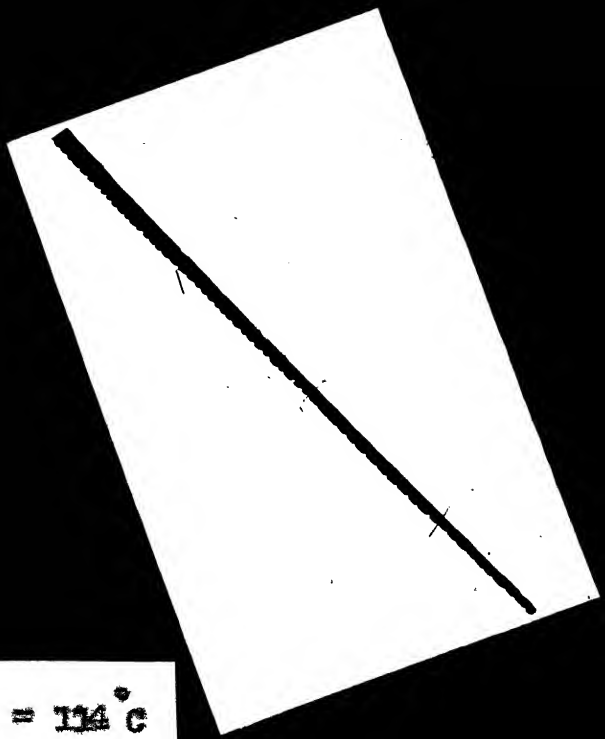

(c) $\theta = 45^{\circ}$, $t_o = 114^{\circ}C$

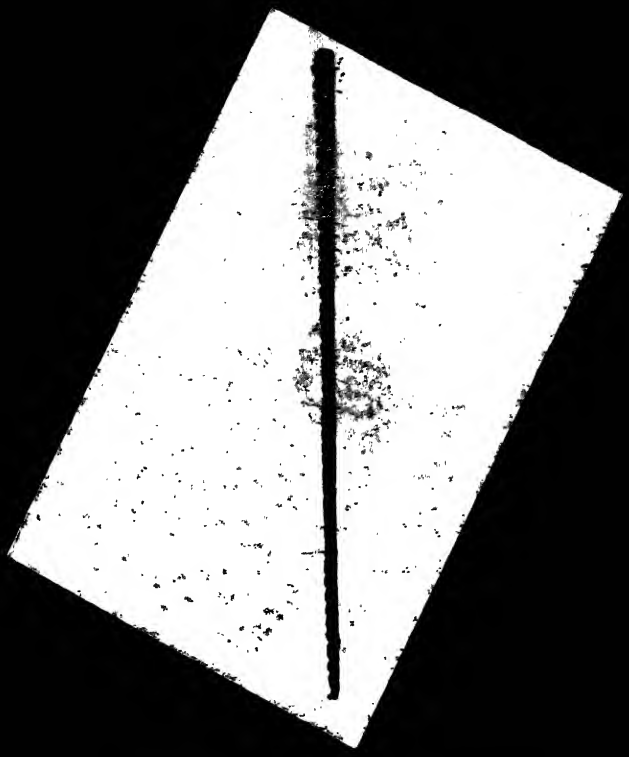

(a) $\theta = 0^{\circ}$, $t_o = 114^{\circ}C$

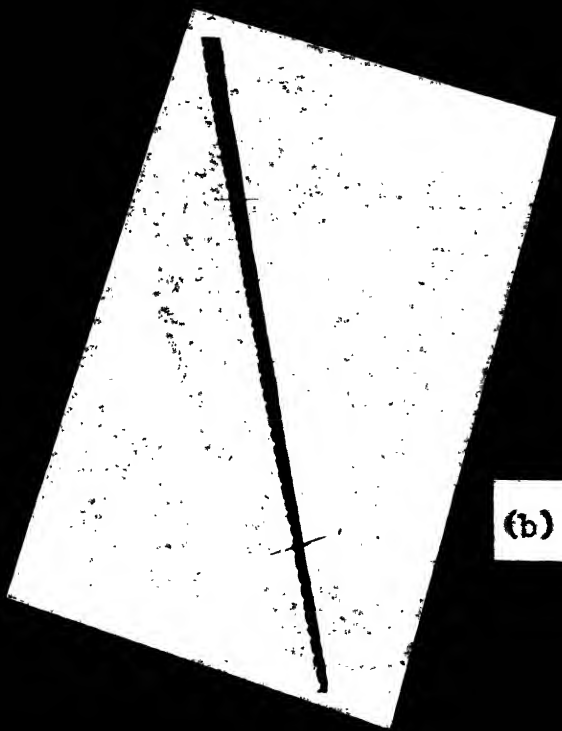

(b) $\theta = 10^{\circ}$, $t_o = 114$

Table 1

θ in degrees	Range of q in watts for the smooth plate	Range of q in watts for the roughened plate with 18 gauge wires	Range of q in watts for the roughened plate with 16 gauge wires
0	27 - 158	26 - 156	60 - 218
10	39 - 120	56 - 162	35 - 176
30	11 - 119	29 - 193	51 - 213
45	16 - 99	26 - 195	40 - 225
60	53 - 141	60 - 150	92 - 255
90	29 - 116	34 - 220	70 - 206

CHAPTER 4

4.1 RESULTS AND DISCUSSION

4.1.1 Temperature Distribution of the Test Plate Surface

Figure (4.1.1) shows the temperature distribution of the smooth plate for the horizontal, inclined ($\theta = 45^{\circ}$) and the vertical orientations. Figures (4.1.2) and (4.1.3) give the temperature distribution for the rough plates, roughened with 18 and 16 gauge wires, respectively.

The temperature around the middle of the plate is slightly higher than that towards the edges. The variation in the surface temperature is, however, within $\pm$ 2 percent of the average temperature of the surface. The surface of the plate is, therefore, assumed to be isothermal.

4.1.2 Schlieren Study

The schlieren photographs, for the vertical and the inclined positions of the heated roughened plate, with 18 gauge wire, are shown in Figure (3.2.2). The temperature of the plate for all the three cases is maintained at $114^{\circ}C$. The boundary layer thickness is seen to increase with increasing distance from the leading edge. With increasing inclination of the test plate to the vertical, the boundary layer is, however, observed to decrease.

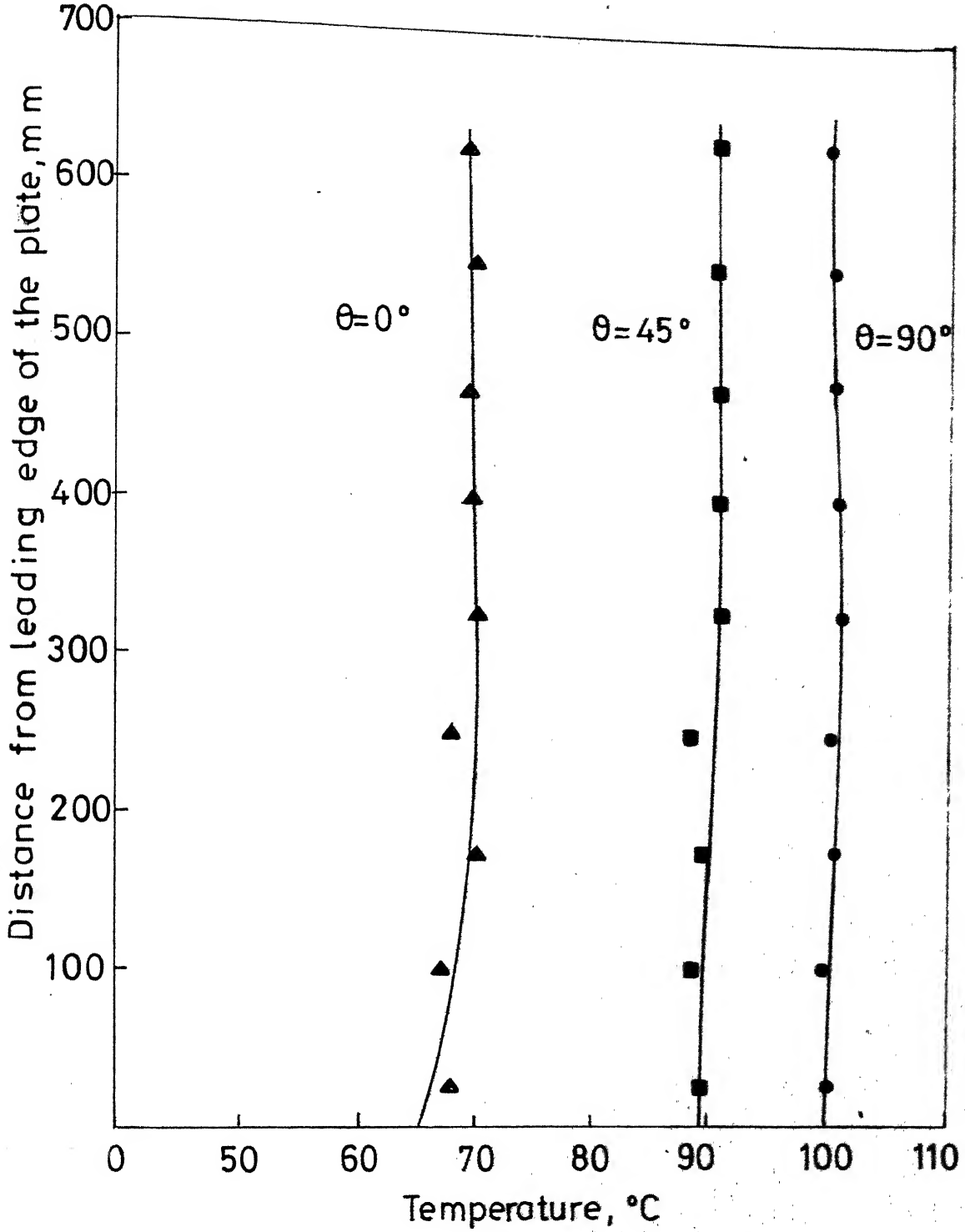

Fig. 4·1·1 Temperature distribution over the smooth plate surface

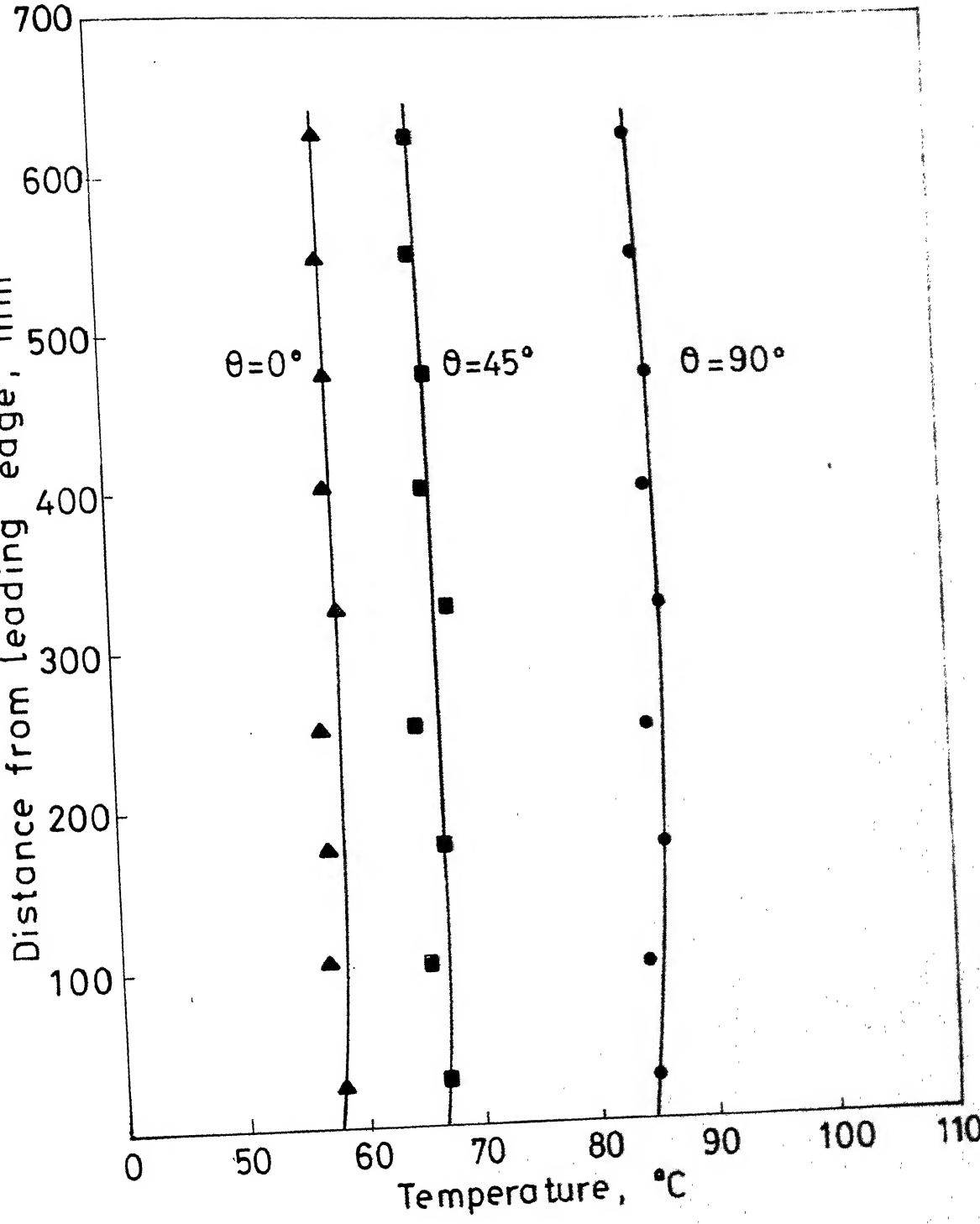

Fig. 4·1·2 Temperature distribution over the rough-plate surface with 18 gauge wire

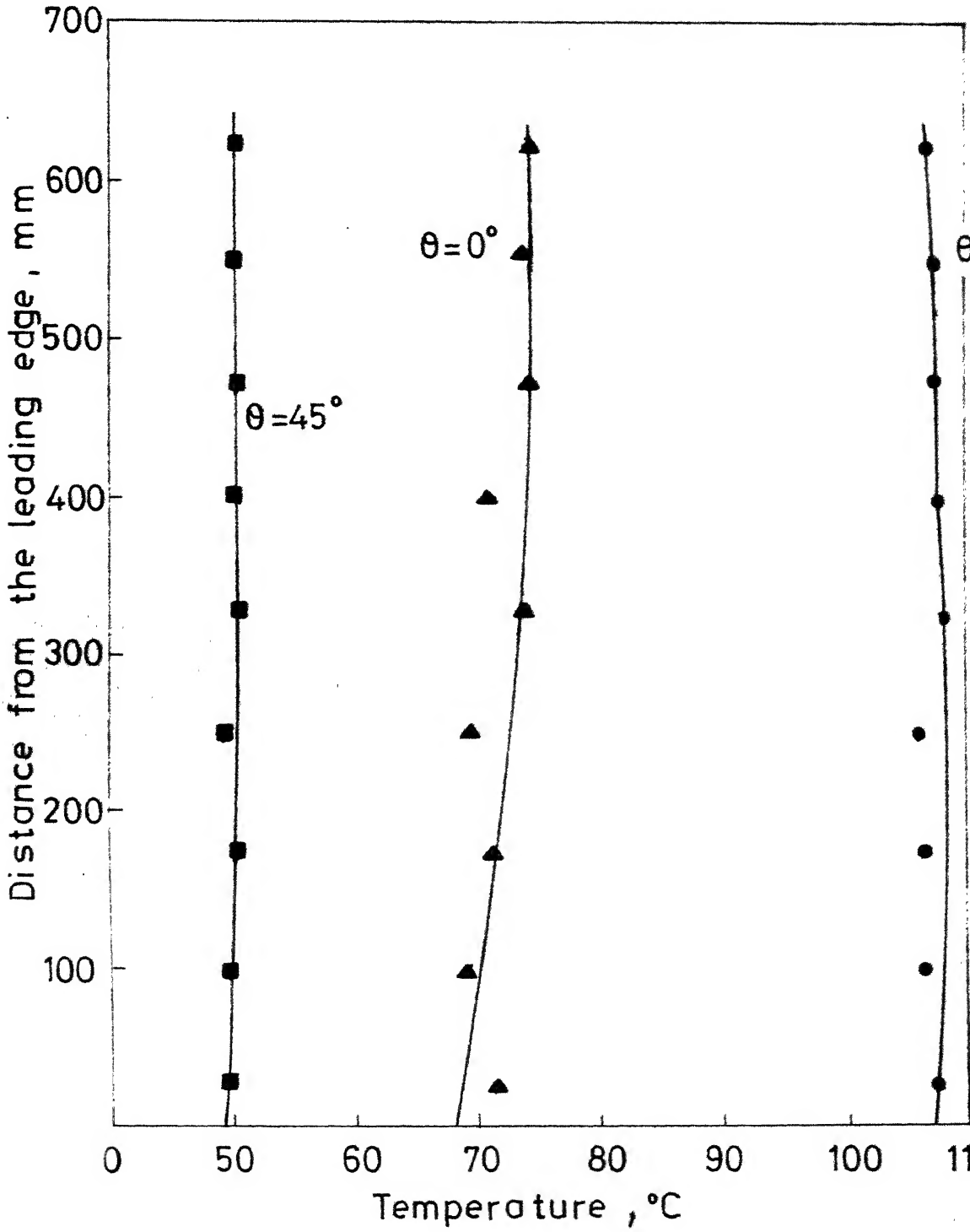

Fig.4·13 Temperature distribution over the rou
plate surface with 16 gauge wire

Figure (3.3.3) shows the schlieren photographs for the vertical and the inclined orientations of the roughened plate using 16 gauge wire. The boundary layer thickness is, as usual, seen to increase along the length of the plate, but in comparison with the 18 gauge roughened plate it is observed to be relatively thinner. This obviously results in increased heat dissipation from the test plate. This effect of enhanced heat transfer due to reduced thickness of the boundary layer is observed to be true for all the inclinations of the 16 gauge roughened plate to the vertical.

4.1.3 Relation Between Average Nusselt Number and Average Rayleigh Number

To correlate the experimental data for the smooth inclined plate an expression of the form $Nu = C\ (Ra\ \cos\theta)^r$ has been considered. The value for the exponent r is taken as 0.25, as recommended by Fujii (3). Based on this value of r and the data obtained from the experiments, the magnitude of constant C in the above equation is evaluated. The expression for the correlation thus developed is as follows.

$$Nu = 0.77\ (Ra\ \cos\theta)^{0.25}$$

Figure (4.1.4) through (4.1.8) show the variation of Nu Vs Ra cosθ for different inclinations of the smooth and the roughened plates. For the inclined smooth plate the slope of the lines passing through

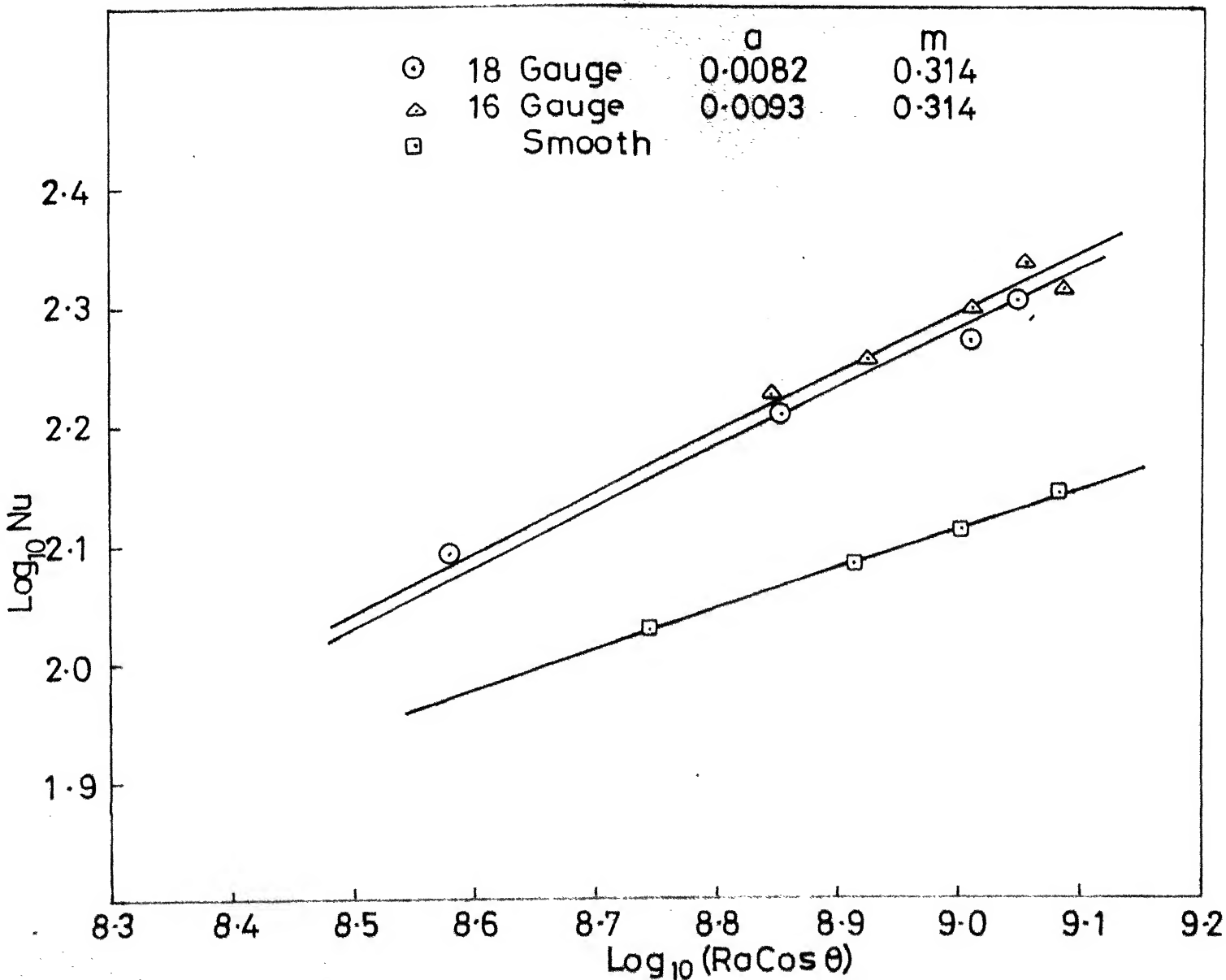
a
m
18 Gauge 0·0082 0·314
16 Gauge 0·0093 0·314
Smooth
2·4
2·3
2·2
2·1
2·0
1·9
Log10 Nu
8·3
8·4
8·5
8·6
8·7
8·8
8·9
9·0
9·1
9·2
Log10 (RaCos θ)

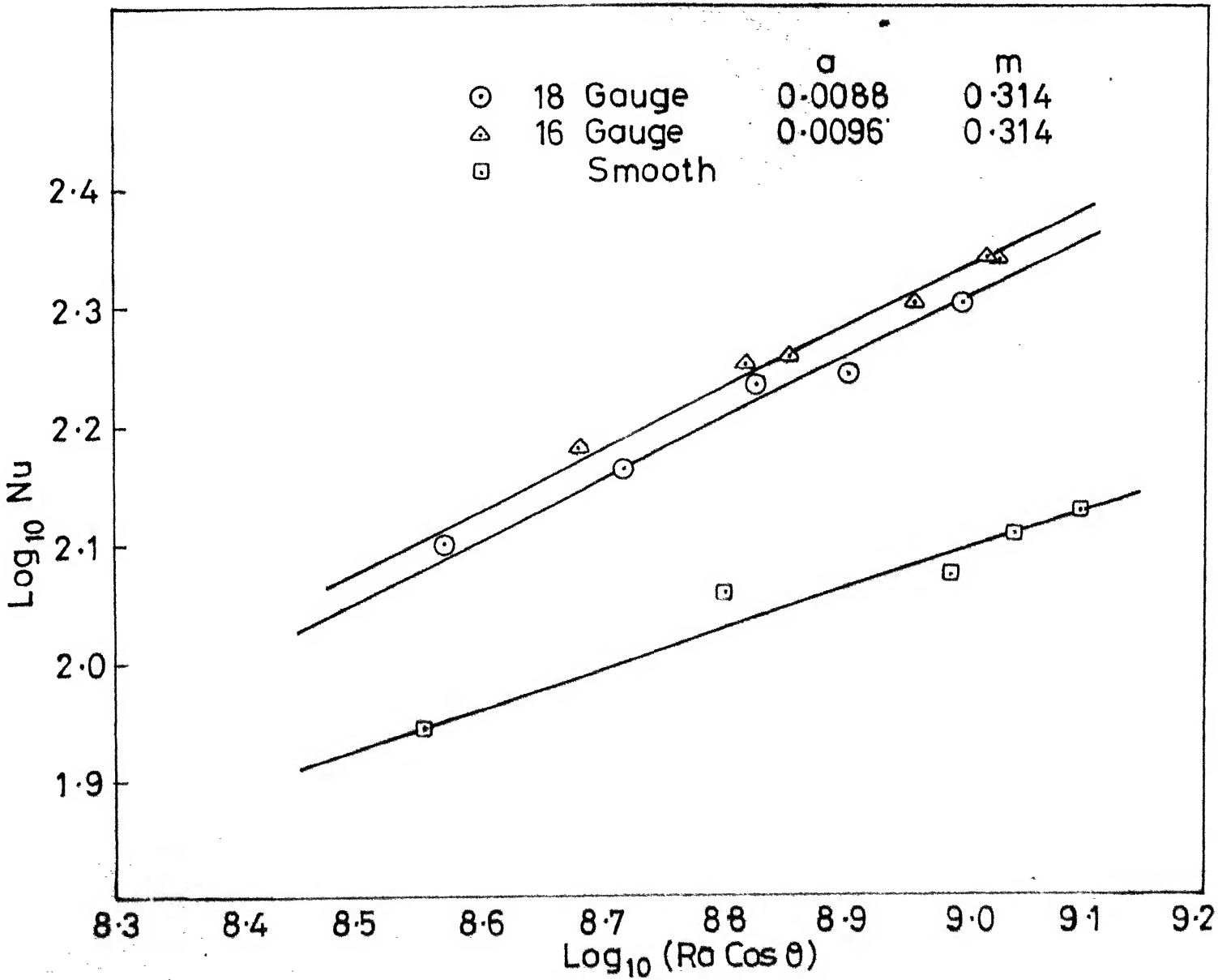
a
m
18 Gauge
0·0088
0·314
16 Gauge
0·0096
0·314
Smooth
2·4
2·3
2·2
2·1
2·0
1·9
Log10 Nu
8·3
8·4
8·5
8·6
8·7
8·8
8·9
9·0
9·1
9·2
Log10 (Ra Cos θ)

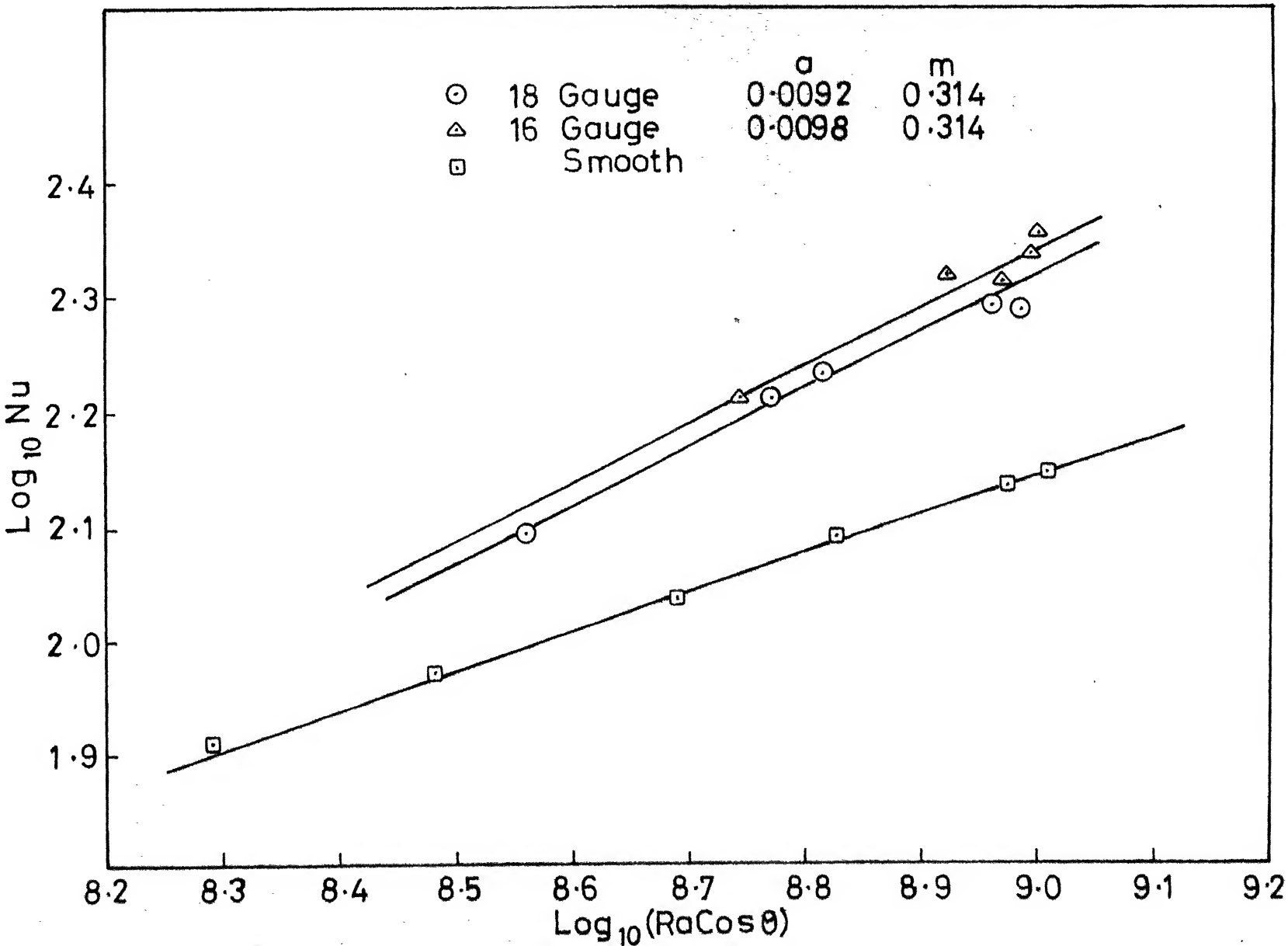
a
m
18 Gauge 0·0092 0·314
16 Gauge 0·0098 0·314
Smooth
2·4
2·3
2·2
2·1
2·0
1·9
Log10 Nu
8·2
8·3
8·4
8·5
8·6
8·7
8·8
8·9
9·0
9·1
9·2
Log10 (RaCos θ)

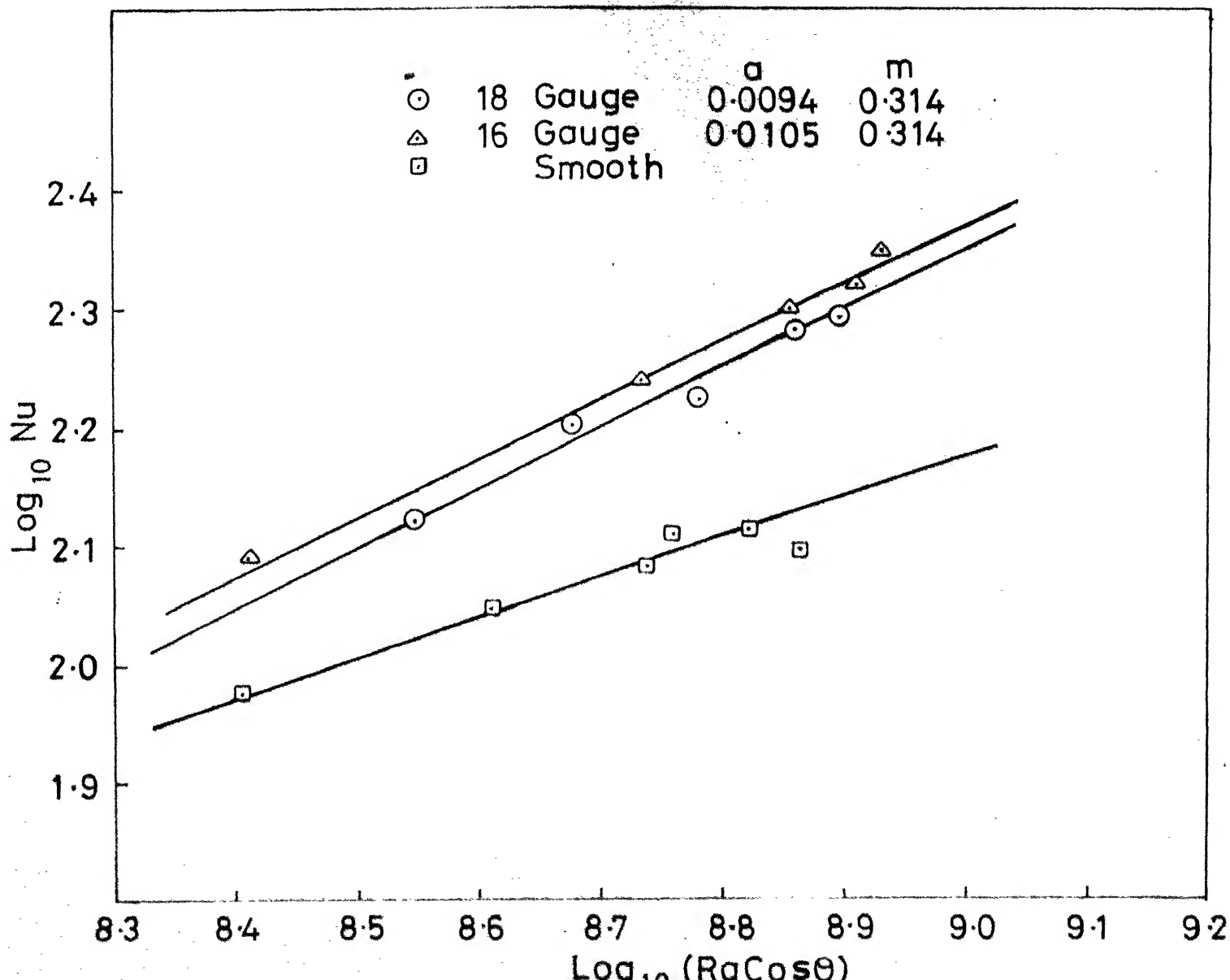
a m
18 Gauge 0·0094 0·314
16 Gauge 0·0105 0·314
Smooth
2·4
2·3
2·2
2·1
2·0
1·9
Log10 Nu
8·3
8·4
8·5
8·6
8·7
8·8
8·9
9·0
9·1
9·2
Log10 (RaCosθ)

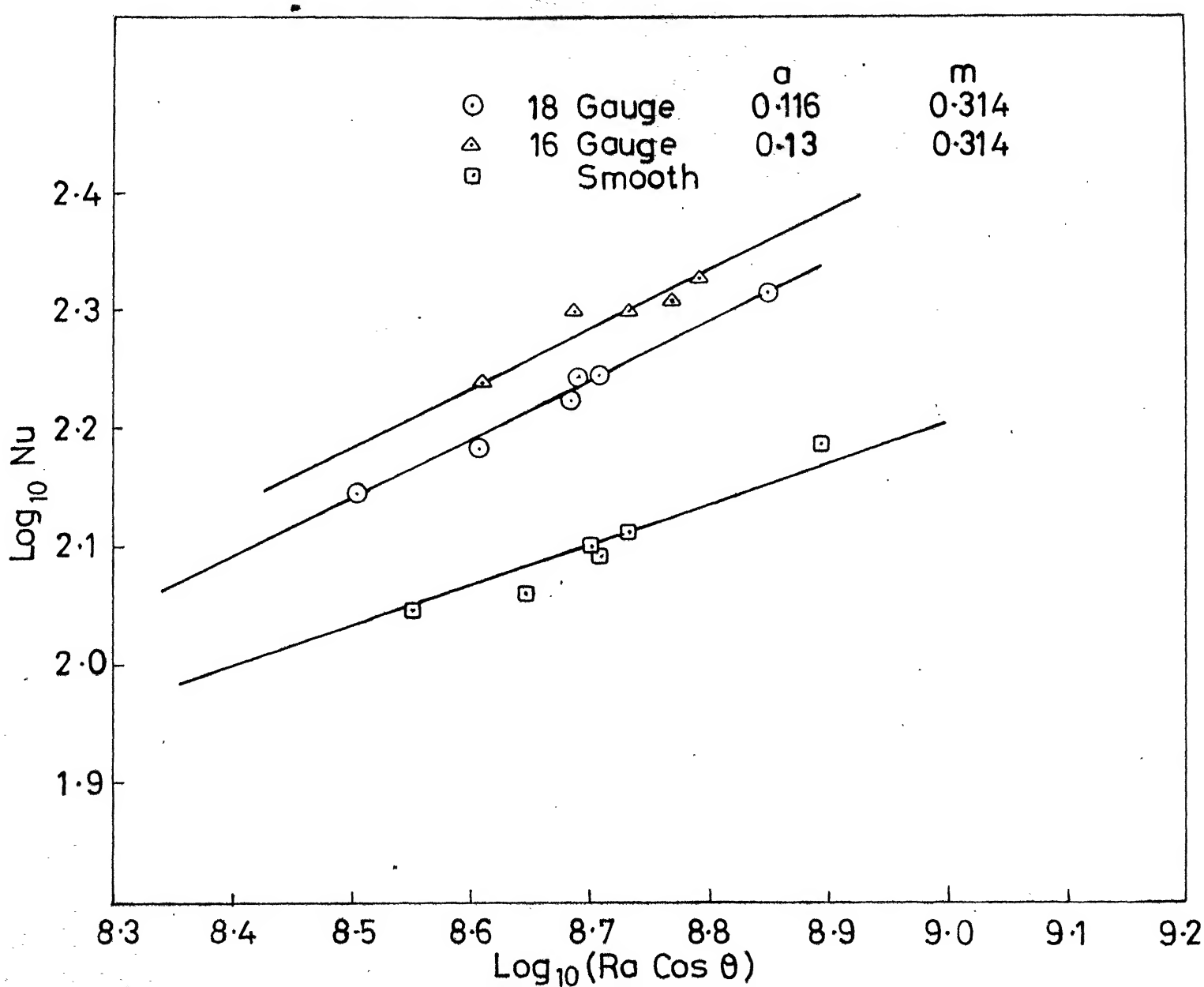
a
m
18 Gauge
0·116
0·314
16 Gauge
0·13
0·314
Smooth
2·4
2·3
2·2
2·1
2·0
1·9
Log10 Nu
8·3
8·4
8·5
8·6
8·7
8·8
8·9
9·0
9·1
9·2
Log10 (Ra Cos θ)

the test points for the various angles of inclination is found to be 0.33. This agrees well with the findings of Fujii (3).

For the inclined roughened plates the slope of the lines passing through the data points for various inclinations is seen to be 0.5, which is higher than that realized for the smooth inclined plates. This magnitude of the slope is further found to be in complete conformity with the value predicted by the integral method analysis, as presented in Chapter 2. To solve Eq. (2.19) for the roughened plates, the value of m is assumed to be 0.314, as suggested by Hopf (14). With this value of m, the value of a is computed for various inclinations and roughnesses of the test plate.

An attempt has been made to correlate the experimental data obtained from both the roughened plates and the correlation is shown in Figure (4.1.10). The figure gives the variation of Ra cosθ vs Nu. With increasing values of Ra cosθ the Nusselt number is found to increase, which means that increased temperature difference, between the plate surface and the ambient surroundings, results in an enhanced heat dissipation from the test plate. The heat loss is also observed to increase with the increasing angle of inclination.

4.2 CONCLUSIONS

(1) It is observed that the turbulent free convective heat transfer rates from smooth inclined plates can be considerably

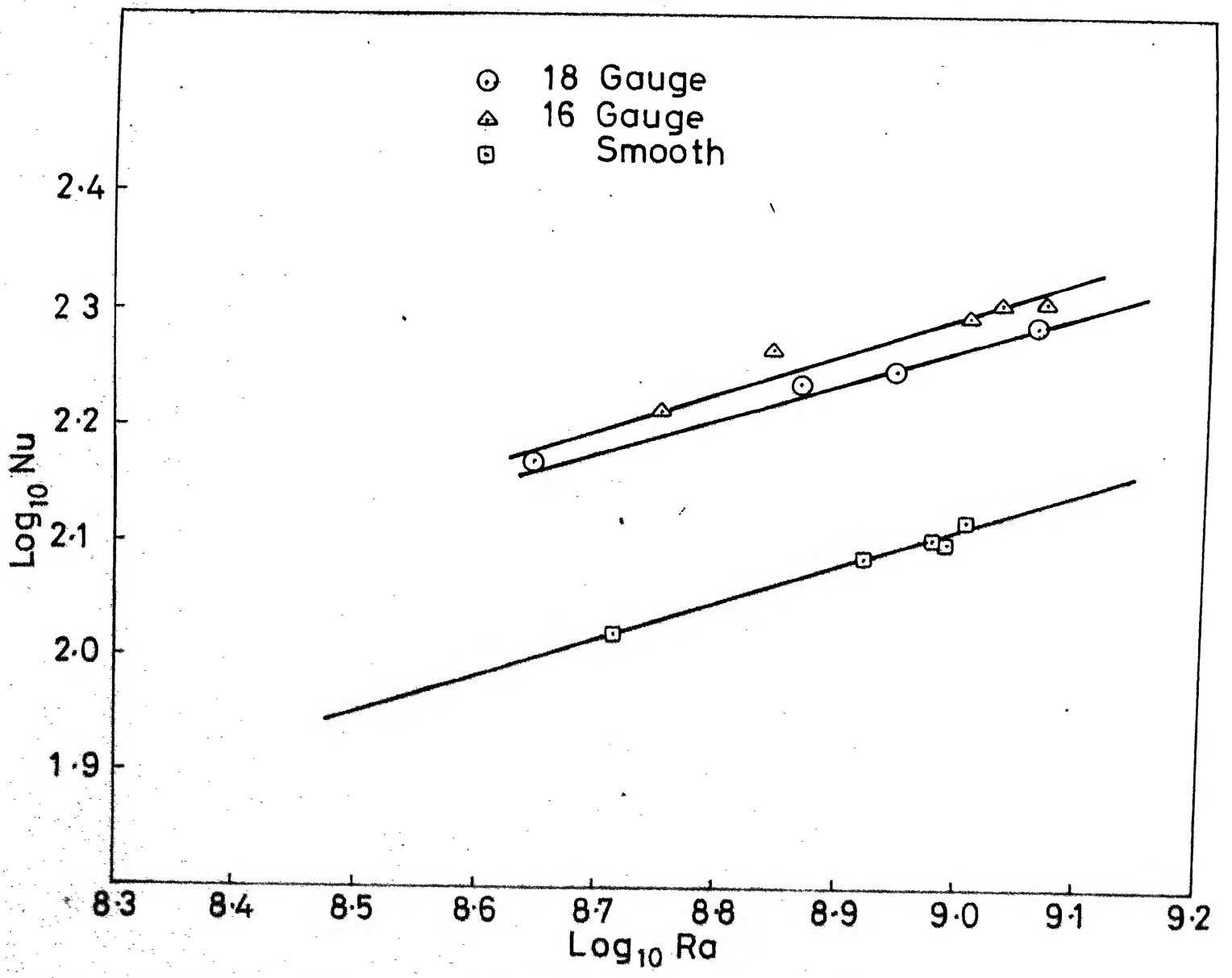

Fig. 4·1·9 Relation of Nu vs Ra for the plate inclined at θ=90°

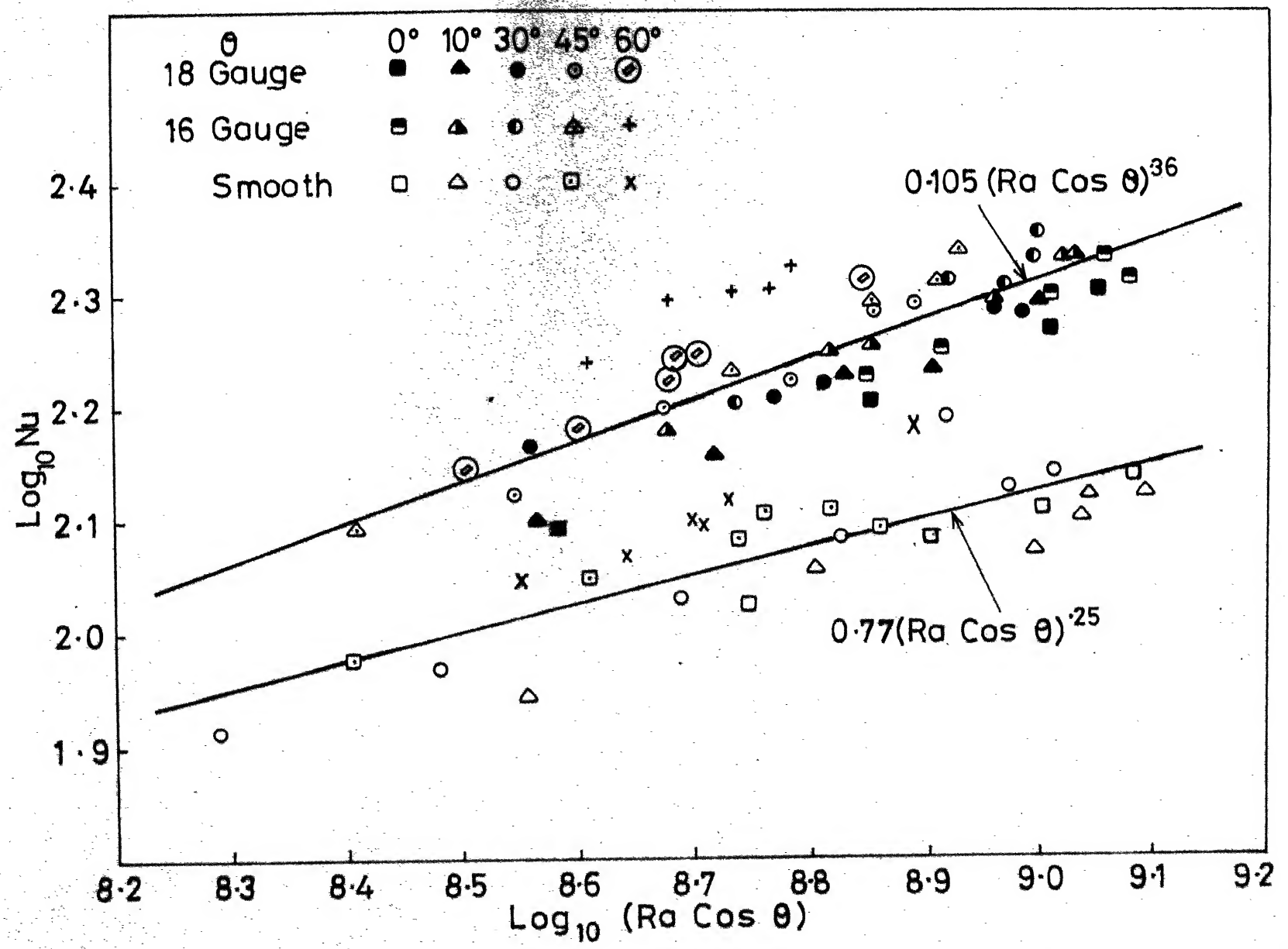
θ
0° 10° 30° 45° 60°
18 Gauge
16 Gauge
Smooth
0·105 (Ra Cos θ)^36
0·77(Ra Cos θ)^·25
Log10 Nu
Log10 (Ra Cos θ)
2·4
2·3
2·2
2·1
2·0
1·9
8·2
8·3
8·4
8·5
8·6
8·7
8·8
8·9
9·0
9·1
9·2

enhanced by artificially roughening the plate surfaces. The augmentation to the free convective heat transfer due to surface roughness in the present investigation is found to be of the order of 35 percent.

(2) In all the cases studied it was observed that the boundary layer is thinner at the leading edge and thicker at the trailing edge. It was also found that the boundary layer thickness decreases with the increase in heat transfer.

(3) The test results also show that natural convection heat transfer from roughened inclined plates facing upwards can be predicted by the correlation $Nu = 0.105\ (Ra \cos\theta)^{0.36}$ within an accuracy of $\pm$ 4 percent.

(4) Natural convection heat transfer from an inclined smooth plate facing upwards can be evaluated by using the correlation

$$Nu = 0.77\ (Ra \cos\theta)^{0.25}$$

However, it is seen that the average heat transfer coefficients yielded by the above proposed relation are 6.5 percent higher than that given by Fujii's (3) correlation. The higher heat transfer coefficients obtained in the present investigation can be explained by the fact that the flow is not restricted to a 2-dimensional configuration, since the plate is open to flow from all sides.

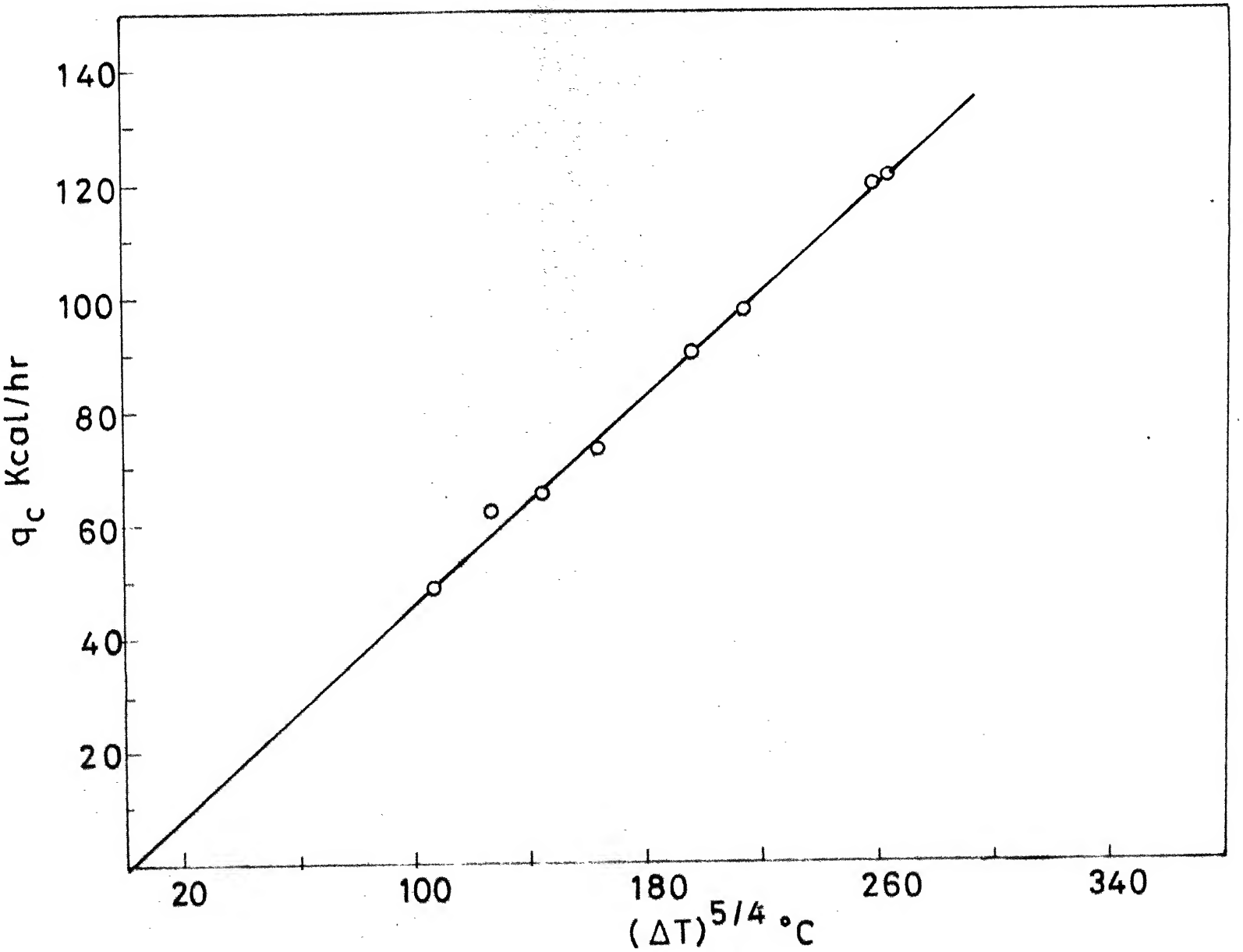
140
120
100
80
60
40
20
q_c Kcal/hr
20
100
180
260
340
$(\Delta T)^{5/4}$ °C

(5) Free convection heat transfer is found to obey the 5/4 power relation, that is $q_c \propto (\Delta T)^{5/4}$.

4.3 SCOPE FOR FUTURE WORK

Since the experimental results from the above study cover only two surface roughnesses and Grashof numbers between 10^8 to 10^9, the scope of the present study is limited. It is therefore essential and desirable to extend the range of application of the above proposed correlation to include large Grashof numbers.

To achieve greater accuracy, the experiments can be carried out on an optical instrument, like a differential interferometer, and the flow restricted to 2-dimensions by attaching optical glass walls to the test plate sides along their lengths. With the help of an interferometer it would also be possible to study the effect of surface roughness on the local heat transfer coefficient.

REFERENCES

1. B.R. RICH; An Investigation of Heat Transfer From an Inclined Plate in Free Convection, TRANS.ASME, Vol. 75, 1953, pp. 489.

2. G.E. VLIET; Natural Convection Local Heat Transfer on Constant Heat Flux Inclined Surfaces, TRANS. ASME, Vol. 91C, 1969, pp. 511.

3. TETSU FUJII AND HIDEAKI IMURA; Natural Convection Heat Transfer From a Plate With Arbitrary Inclination, Int. J. Heat and Mass Transfer, Vol. 15, 1972, pp. 755.

4. W.Z. BIACK AND J.K. NORRIS; The Thermal Structure of Free Convection Turbulence From Inclined Isothermal Surfaces and Its Influence on Heat Transfer, Int.J. Heat and Mass Transfer, Vol. 18, 1975, pp. 43.

5. J.NIKURADSE; Laws of Flow in Rough Pipes, VDI-Forschungsheft 361, Series B, 4 (1933), NACA TM 1292, 1950.

6. L.M.K. BOELTER, G.YOUNG, V.D. SANDERS, M. MARGAN AND M.L. GREENFIELD; Experimental Determination of Thermal and Hydrodynamical Behaviour of Air Flowing Along Flat Plate Containing Turbulence Promoters, NACA Rep. 2517, 1951.

7. W. NUNNER; Heat Transfer and Pressure Drop in Rough Tubes, V.D.I. Forschungsheft 455, Supplement to Forschung anf dem Gebiete des Ingenieur - Wesens, R. Vol. 22, 1956, pp. 5.

8. F.J. EDWARDS AND N.SHERIFF; The Heat Transfer and Friction Characteristics for Forced Convection Air Flow Over Particular Type of Rough Surface, International Developments in Heat Transfer ASME Part III, Paper 45, 1961, pp. 415.

9. V. GOMELAURI; The Influence of Artificial Roughness on Convective Heat Transfer, Int. J. Heat and Mass Transfer, Vol. 7, 1964, pp. 653.

10. N. SHERIFF; P. GUMLEY AND J. FRANCE ; Heat Transfer Characteristics of Roughened Surface, Chem. Proc. Engg. Vol. 45, 1964, pp. 624.

11. R.A. GOWEN; J.W. SMITH; Turbulent Heat Transfer from Smooth and Rough Surfaces, Int. J. Heat and Mass Transfer Vol. 11-2, 1968, pp. 1957.

12. A.J. EDE; Advances in Free Convection, Advances in Heat Transfer, Academic Press Vol. 4, 1967.

13. E.S.R.G. ECKERT AND T.W. JAKSON; Analysis of Turbulent Free Convection Boundary Layer on Flat Plate, NACA Rep. 1015, 1951.

14. L.Z. HOPF; Angew, Math. V. Mech. Vol. 3, 1923, pp. 329.

15. K.Z. FROMM; Angew, Math. V. Mech. Vol. 3, 1923, pp. 339.

16. MAX JACOB ; Heat Transfer Vol. 1, John Wiley and Sons, New York pp. 567.

17. HERMANN SCHLICHTING; Boundary Layer Theory, McGraw-Hill, New York, pp. 551.

18. ROHSENOW AND HARTNETT; Hand Book of Heat Transfer, McGraw-Hill, New York.

19. KOTHANDARAMAN AND SUBRAMANYAN; Heat and Mass Transfer Data Book, Wiley Eastern, Pvt. Ltd. India.

20. JAMES KNUDSEN AND DONALD KATZ; Fluid Dynamics and Heat Transfer, McGraw-Hill, New York, pp. 174.

21. BENJAMIN GEBHART; Heat Transfer, Tata McGraw-Hill, Bombay, pp. 361.

APPENDIX-A

THERMOCOUPLE CALIBRATION

Thermocouple is an important, accurate and stable temperature measuring device with rapid response and low maintenance cost. It consists of two dissimilar electrical conductors either or both of which may be pure metals, alloys or non-metals, having a common junction where the conductors are in good thermal and electrical contact. Common types of thermocouples are copper-constantan, iron-constantan, chromel-alumel etc. and their selection for a particular use depends upon various factors like range of temperature measurements needed and the type of atmosphere surrounding the measuring junction. For the present work chromel-alumel thermocouples have been chosen.

Measurement of temperature by means of thermocouple is based on the simple fact that when two junctions formed by two dissimilar conductors are maintained at different temperatures, a small electromotive force is generated in the circuit, the magnitude of which depends upon the temperature difference between the junctions. Every thermocouple bears a certain relationship between the temperature difference of the two junctions and the electromotive force generated in the circuit.

The simplest thermocouple circuit arrangement is shown in Figure A-1. One of the junctions called the cold junction (or the

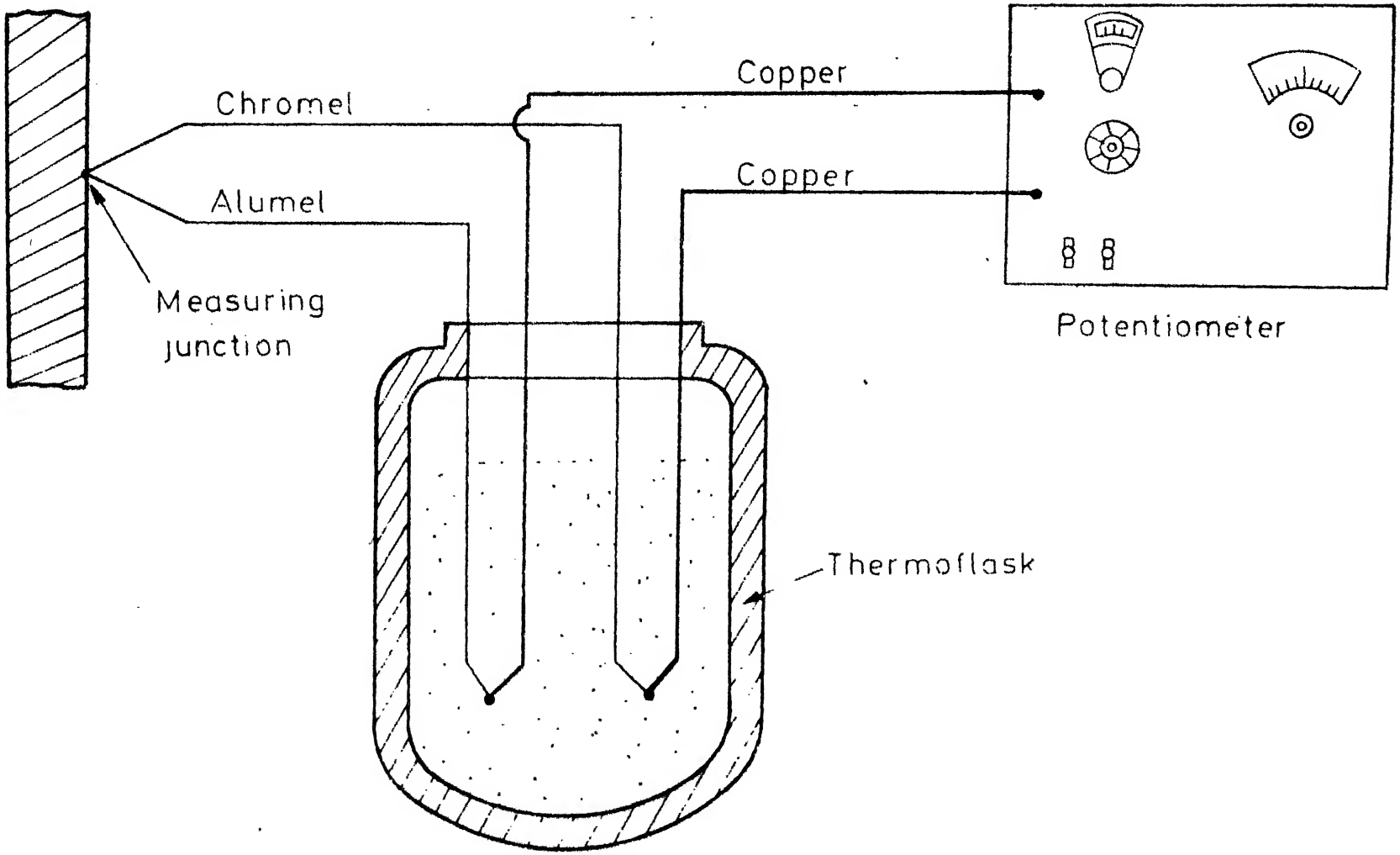

FIG. A-1 THERMOCOUPLE CIRCUIT

reference junction) is maintained at a fixed known temperature (usually ice point), and the other junction known as the hot junction is inserted into the unknown temperature bath. The thermocouple may be lengthened, to remove the effective cold junction from the influence of the heated zone either by adding compensating leads made from materials identical to those of the thermocouple or by forming a thermocouple pair of similar emf characteristics over the range of temperature to which the ends of the compensating leads are likely to be exposed. A sensitive and accurate millivolt potentiometer may be used to measure the emf generated in the circuit and by using the relationship between the temperature difference between the two junctions and the emf developed in a particular thermocouple, the unknown temperature is calculated.

The temperature-emf relationship of a thermocouple depends upon the type of metals used. (In the manufacture of thermocouples it is inevitable that some impurities will be present in quite appreciable proportions). Moreover, this relationship depends upon the ways in which the junctions are made and the type of lead wires used for connecting the thermocouples to the emf measuring device. Therefore, whenever high accuracy is desired, proper calibration of thermocouples is necessary.

Since all the thermocouples used in the experiment are drawn from the same lot, are of equal length and have the same length and

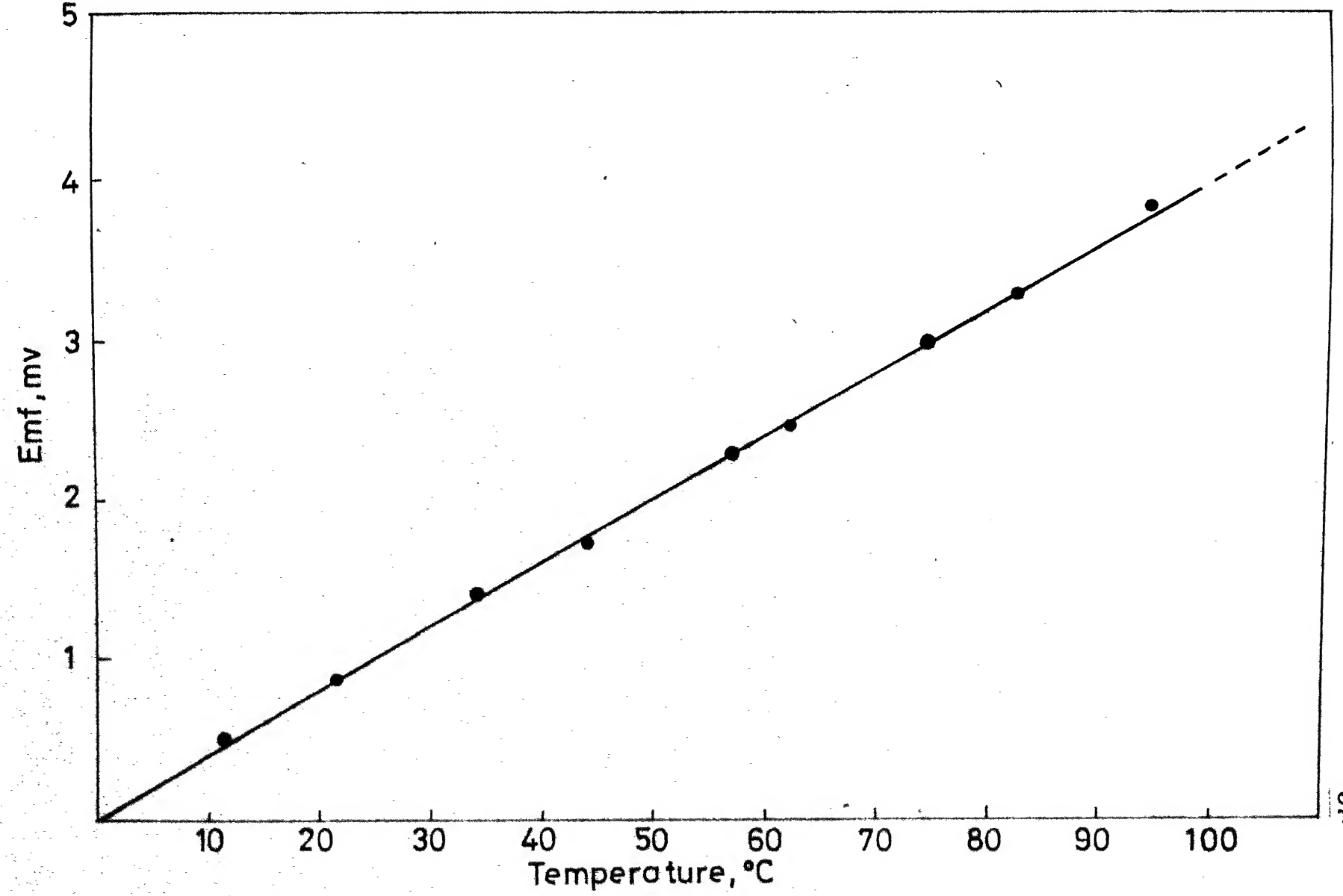
5
4
3
2
1
Emf, mv
10
20
30
40
50
60
70
80
90
100
Temperature, °C

size of copper extension wires it is decided to calibrate only half of them.

The hot junction of thermocouple is placed in an electrically heated, temperature controlled, and stirred water bath. A standard mercury-in-glass thermometer graduated in $1/10^{ths}$ of a degree is used to indicate the bath temperature. The thermocouple emf is measured with a Leeds and Northrup millivolt pctentiometer. A number of readings are taken by maintaining the water bath at various temperature levels.

To maintain the cold junction of thermocouple at ice point an equilibrium solution of crushed ice and distilled water is taken into a thermos flask. From time to time ice is added and the mixture is stirred thoroughly by means of a glass rod to ensure it solution temperature of $0^{o}C$. An accurate thermometer is also inserted into the cold junction thermos flask to check the constancy of temperature of melting ice inside it. The calibration curve is shown in Figure A-2.

APPENDIX B

For the calculation of Nusselt number an estimate of heat transfer is necessary and this can be achieved by carrying out a heat balance analysis. There are two modes of heat transfer in the system,

i) heat lost by convection

ii) heat lost by radiation.

Convective heat transfer rate from the test surface is calculated by the subtraction of radiation loss from the surface together with the total losses from the sides from the energy input to the main heater. The backward loss is neglected because of the guard heater arrangement.

If q_c is the heat transfer from the test surface due to convection alone, then

$$q_c = h_{avg} A (t_o - t_\infty) \quad \text{and} \quad h_{avg} = \frac{q_c}{(t_o - t_\infty) A}$$

Therefore, $Nu = \frac{h_{avg} L}{K}$

The radiative heat loss from the sides being very small is neglected. However, the convective heat loss from the sides, does not exceed 4 percent of total power input to the main heater.

Calculation of Grashof Number

Average temperature of the test

plate surface = 144°C

Ambient temperature = 32.9°C

Mean film temperature = 88.25°C

Temperature of the room wall = 33°C

Properties of air at the mean film temperature

$K = .024$ Kcal/hr-m-°C

$Pr = .7$

$\nu = 21.9 \times 10^{-6}$ m^2/sec

$$\therefore \quad Gr = \frac{9.81 \times 111.5 \times (.65)^3 \times 10^{12}}{361.25 \times (21.9)^2}$$

$$= 12.25 \times 10^8$$

$Ra = Gr \times Pr$

$$= 12.25 \times .7 \times 10^8$$

$$= 8.575 \times 10^8$$

Calculation of Nusselt Number

Heat input = Heat lost by convection from the test plate + Heat lost by radiation from the test plate + convective heat loss from the sides.

Heat lost by radiation from test plate,

$$q_r = \varepsilon_a \ \sigma A \ (T_0^4 - T_w^4)$$

where $\sigma = 4.9 \times 10^{-8}$

$$\varepsilon_a = .05$$

$$q_r = 4.9 \times .31 \times .65 \times .05 \left[\left(\frac{417}{100}\right)^4 - \left(\frac{306}{100}\right)^4\right]$$

$$= 10.5 \quad \text{Kcal/hr}$$

Since the heat lost from the exposed side surfaces of the test plate is found to be of the order of 4 percent of the energy input to the main heater, therefore the total heat lost from the sides is computed as follows

$$= .04 \times (.226 \times 860)$$

$$= 7.8 \quad \text{Kcal/hr}$$

$$q_c = 195 - 10.5 - 7.8 = 176.7$$

$$Nu = \frac{176.7 \times .65}{(.65 \times .31) \times 111.5 \times .024}$$

$$= 221.24$$